Supporting Information

Novel quinoline-based Ir(III) complexes exhibit high antitumor activity *in vitro* and *in vivo*

Yan Yang,[a,b,1] Yi-Dong Bin,[a,b,1] Qi-Pin Qin, [a,d]* Xu-Jian Luo [a], Bi-Qun Zou, [c,d]* and Hua-Xin Zhang [b]*

EXPERIMENTAL SECTION

General experimental details

Synthesis

Solvents were purchased from ALADDIN. Infrared spectra were recorded with a Perkin Elmer Spectrum One FT IR Spectrometer; ^{1}H NMR and ^{13}C NMR spectra were recorded at Bruker DRX 500NMR spectrometer , chemical shifts are given in ppm relative to internal tetramethylsilane.Mass spectrum were recorded with Thermo□Finngan LCQ/AD Quadrupole Ion Trap ESI MS.

Synthesis of main ligand. The 6,7-Dichloro-5,8-quinolinequinone[1] and pyrido [3,2-a] pyrido [1',2':1,2] imi-dazo [4,5-c] phenazine **(P)**, 12,13-dimethylpyrido [3,2-a] pyrido [1',2':1,2] imidazo [4,5-c] phenazine **(dMP)**, 2-methylpyrido [3,2-a] pyrido [1',2':1,2] imidazo [4,5-c] phenazine **(MP)**, 2,12,13-trimethylpyrido [3,2-a] pyrido [1',2':1,2] imidazo [4,5-c] phenazine **(tMP)** were synthesized as previously reported [2].These compounds were characterized by ^{1}H NMR, IR and ESI-MS.

Data for **P:** IR (KBr): 3297.23, 3047.96, 1623.39, 1527.17, 1438.71, 1374.13, 1341.86, 1277.91, 1245.43, 1004.11, 746.45, 698.01, 757.97, 609.54. ^{1}H NMR (500 MHz, Chloroform-d) δ 10.37 (d, J = 6.5 Hz, 1H, H_1), 9.67 (d, J = 8.0 Hz, 1H, H_8), 9.25 (d, J = 3.5 Hz, 1H, H_3), 8.38 (t, J = 8.0 Hz, 2H, H_4 and H_7), 8.29 (s, 1H, H_2), 7.93 (dt, J = 24.1, 7.2 Hz, 2H, H_5 and H_6), 7.80 – 7.70 (m, 2H, H_{10} and H_{11}), 7.37 (t, J = 6.3 Hz, 1H, H_9). ESI-MS m/z: Calculated ms: 321.10, found: 321.19 $[M]^+$. Elemental analysis calcd (%) for $C_{20}H_{11}N_5$: C 74.76, H 3.45, and N 21.79; found: C 74.75, H 3.47, and N 21.78.

Data for **dMP:** IR (KBr): 3027.91, 2961.11, 1584.37, 1526.88, 1450.58, 1407.11, 1413.68, 1339.70, 1278.40, 1014.91, 863.86755.75, 705.23, 422.67. ^{1}H NMR (500 MHz, Chloroform-d) δ 10.39 (d, J = 7.8 Hz, 1H, H_1), 10.33 (d, J = 6.7 Hz, 1H, H_8), 9.64 (d, J = 8.0 Hz, 1H, H_3), 9.20 (d, J = 4.0 Hz, 1H, H2), 8.12 (d, J = 11.3 Hz, 2H, H_4 and H_7), 8.06 (d, J = 9.1 Hz, 1H, H_{11}), 7.73 (d, J = 12.5 Hz, 1H, H_{10}), 7.63 – 7.58 (m, 1H, H_9), 2.62 (s, 3H, H_5), 2.62 (s, 3H, H_6). ESI-MS m/z: Calculated ms: 349.13, found: 350.44 $[M+H]^+$. Elemental analysis calcd (%) for $C_{22}H_{15}N_5$: C 75.63, H 4.33, and N 20.04; found: C 75.62, H 4.34, and N 20.02.

Data for **MP:** IR (KBr): 3064.84, 2555.09, 2271.66, 1911.06, 1706.11, 1575.48, 1539.75, 1449.69, 1398.93, 1327.62, 1258.47, 1095.66, 1015.51, 832.81, 755.73, 709.32, 586.13. ^{1}H NMR (500 MHz, Chloroform-d) δ 10.06 (s, 1H, H_1), 9.62 (d, J = 8.1 Hz, 1H, H_8), 9.23 – 9.17 (m, 1H, H_3), 8.34 (dd, J = 7.6, 5.2 Hz, 2H, H_4 and H_7), 8.03 (d, J = 9.0 Hz, 1H, H_2), 7.91 (t, J = 7.6 Hz, 1H, H_5), 7.86 (t, J = 7.5 Hz, 1H, H_6), 7.72 (dd, J = 8.0, 4.5 Hz, 1H, H_{10}), 7.50 (d, J = 9.1 Hz, 1H, H_{11}), 2.62 (s, 3H, H_9). ESI-MS m/z: Calculated ms: 335.12,

found: 335.72 $[M]^+$. Elemental analysis calcd (%) for $C_{21}H_{13}N_5$: C 75.21, H 3.91, and N 20.88; found: C 75.20, H 3.94, and N 20.86.

Data for **tMP:** IR (KBr): 3033.85, 2961.14, 2915.57, 1634.75, 1584.06, 1527.27, 1450.37, 1403.69, 1327.39, 1278.82, 1203.39, 1126.36, 1095.32, 832.60, 709.63, 583.91. ^{1}H NMR (500 MHz, Chloroform-d) δ 9.72 (s, 1H, H_1), 9.38 (d, J = 8.1 Hz, 1H, H_8), 9.12 (d, J = 3.1 Hz, 1H, H_3), 7.90 (d, J = 9.1 Hz, 1H, H_4), 7.81 (s, 1H, H_7), 7.77 (s, 1H, H_2), 7.60 (dd, J = 8.0, 4.4 Hz, 1H, H_{11}), 7.38 (d, J = 9.1 Hz, 1H, H_{10}), 2.53 (s, 3H, H_5), 2.50 (s, 3H, H_6), 2.48 (s, 3H, H_9). ESI-MS m/z: Calculated ms: 363.15, found:364.23 $[M+H]^+$. Elemental analysis calcd (%) for $C_{23}H_{17}N_5$: C 76.01, H 4.71, and N 19.27; found: C 76.00, H 4.73, and N 19.26.

Synthesis of eight* Ir(III) *complexes. Synthesis of dimer complex $[Ir(H\text{-}Py)_2Cl]_2$ and $[Ir(MPy)_2Cl]_2$ were prepared according to literature methods. The Ir(III) complexes were synthesized by reacting two equivalents of ligand L with the Ir(III) chloro-bridged dimer [3].

Ir(III) complexes were prepared by the same general method: A mixture of ligand L (0.2 mmol) and $[Ir(H\text{-}Py)_2Cl]_2$/$[Ir(MPy)_2Cl]_2$ (0.1 mmol) in ethylene glycol (20 mL) was refluxed under an inert atmosphere of nitrogen for 10 h. Upon cooling, an aqueous solution of ammonium hexafluorophosphate (excess) was added and the filtrate was reduced in volume by rotary evaoration until precipitation of the crudeproduct occurred. The solid was then filtered and was washed with water and ethanol.and it was stirred for 1h and then evaporated to dryness. The crude product was dissolved in CH_3CN and purified by column chromatography (aluminium oxide). After elution of unreacted organics with CH_2Cl_2 the product was eluted as the only orange fraction with CH_2Cl_2/CH_3CN (5:1 v/v). These complexes were characterized by IR, elemental analyses, HPLC, ^{1}H NMR, ^{13}C NMR and ESI-MS.

Data for **PyP-Ir**: IR (KBr): 3662, 3047, 2921, 2852, 2357, 1605, 1579, 1537, 1421, 1326, 1268, 1282, 1158, 1110, 1058, 1021, 841, 758, 558. ^{1}H NMR (500 MHz, DMSO-d_6) δ 10.12 (d, J = 5.2 Hz, 1H, H_9), 9.67 (d, J = 4.9 Hz, 1H, H_{16}), 8.55 (d, J = 5.5 Hz, 1H, H_{11}), 8.53 – 8.47 (m, 1H, H_{10}), 8.26 (d, J = 5.6 Hz, 2H, H_1 and $H_{1'}$), 8.23 – 8.15 (m, 2H, H_5 and $H_{5'}$), 8.12 (d, J = 4.5 Hz, 2H, H_4 and $H_{4'}$), 7.97 (d, J = 5.2 Hz, 3H, H_{12}, H_{15} and H_{19}), 7.87 (s, 2H, H_6 and $H_{6'}$), 7.82 (s, 1H, H_{13}), 7.76 (d, J = 5.3 Hz, 1H, H_{14}), 7.64 (d, J = 6.8 Hz, 1H, H_{18}), 7.14 (d, J = 5.7 Hz, 2H, H_3 and $H_{3'}$), 7.11 – 6.93 (m, 4H, H_7, $H_{7'}$,H_8 and $H_{8'}$), 6.59 – 6.42 (m, 2H, H_2 and $H_{2'}$), 6.42 – 6.34 (m, 1H, H_{17}). ^{13}C NMR (126 MHz, DMSO-d6) δ 167.41, 167.26, 151.85, 150.77, 150.28, 148.30, 145.38, 145.06, 144.73, 141.28, 140.03, 139.07, 137.11, 136.21, 133.60, 133.02, 132.40, 131.72, 131.56, 131.15, 130.55, 130.18, 129.24, 128.01, 127.27, 125.45, 125.20, 124.34, 124.20, 122.95, 122.84, 120.13, 116.65, 114.39. ESI-MS m/z: Calculated ms: 822.19, found: 822.10 $[M\text{-}PF_6]^+$. Elemental analysis calcd (%) for $C_{45}H_{35}F_6IrN_7P$: C 53.46, H 3.49, and N 9.70; found: C 53.44, H 3.52, and N 9.68.

Data for **PydMP-Ir**: IR (KBr): 3661, 3051, 2929, 2853, 2347, 1634, 1606, 1531, 1475, 1437, 1324, 1259, 1137, 1025, 837, 762, 556. ^{1}H NMR (500 MHz, DMSO-d_6) δ 9.90 – 9.80 (m, 1H, H_9), 9.33 (d, J = 7.3 Hz, 1H, H_{16}), 8.38 (d, J = 8.1 Hz, 1H, H_{12}), 8.30 (d, J = 8.3 Hz, 1H, H_{15}), 8.24 – 8.16 (m, 2H, H_1 and $H_{1'}$), 8.07 (t, J = 8.9 Hz, 3H, H_{11}, H_5 and $H_{5'}$), 7.99 (dd, J = 19.6, 7.7 Hz, 2H, H_4 and $H_{4'}$), 7.88 (d, J = 6.8 Hz, 2H, H_6 and $H_{6'}$), 7.81 – 7.74 (m, 1H, H_{10}), 7.65 – 7.55 (m, 2H, H_3 and $H_{3'}$), 7.21 (t, J = 7.3 Hz, 2H, H_7 and $H_{7'}$), 7.14 (t, J = 7.5 Hz, 1H, H_{19}), 7.06 (dt, J = 11.2, 7.5 Hz, 2H, H_8 and $H_{8'}$), 6.96 (t, J = 6.5 Hz, 1H, H_{18}), 6.49 (t, J = 8.2 Hz, 2H, H_2 and $H_{2'}$), 6.35 (d,

J = 9.1 Hz, 1H, H_{17}), 2.56 (s, 3H, H_{13}), 2.40 (s, 3H, H_{14}). ^{13}C NMR (126 MHz, DMSO-d6) δ 167.25, 151.74, 150.59, 147.94, 145.47, 145.04, 143.94, 141.91, 139.28, 139.21, 139.10, 138.56, 135.70, 135.12, 133.37, 132.54, 131.80, 130.54, 127.54, 127.44, 127.27, 125.49, 125.25, 124.17, 123.10, 120.39, 120.12, 116.10, 114.36, 20.67, 20.43. ESI-MS m/z: Calculated ms: 850.21, found: 850.80 $[M\text{-}PF_6]^+$. Elemental analysis calcd (%) for $C_{47}H_{39}F_6IrN_7P$: C 54.33, H 3.78, and N 9.44; found: C 54.30, H 3.82, and N 9.42.

Data for **PyMP-Ir**: IR (KBr):3670,3051,2910,2356,1606,1540,1425,1409,1315,1259,1105,1099,1043,1015,837,771,566. ^{1}H NMR (500 MHz, DMSO-d_6) δ 9.91 (s, 1H, H_9), 9.64 (d, J = 8.0 Hz, 1H, H_{16}), 8.61 (d, J = 8.5 Hz, 1H, H_{11}), 8.48 (d, J = 8.5 Hz, 1H, H_{10}), 8.29 – 8.23 (m, 2H, H_1 and $H_{1'}$), 8.21 – 8.14 (m, 2H, H_5 and $H_{5'}$), 8.09 (dd, J = 8.0, 5.3 Hz, 2H, H_4 and $H_{4'}$), 8.00 – 7.92 (m, 3H, H_{19}, H_6 and $H_{6'}$), 7.87 (td, J = 7.5, 3.5 Hz, 2H, H_3 and $H_{3'}$), 7.81 (d, J = 5.8 Hz, 1H, H_{12}), 7.65 (d, J = 9.3 Hz, 1H, H_{15}), 7.14 (t, J = 7.5 Hz, 1H, H_{13}), 7.03 (ddt, J = 38.9, 16.7, 7.7 Hz, 5H, H_{14}, H_7, $H_{7'}$, H_8 and $H_{8'}$), 6.42 (dd, J = 15.0, 7.5 Hz, 2H, H_2 and $H_{2'}$), 6.27 (d, J = 9.3 Hz, 1H, H_{18}), 2.55 (s, 3H, H_{17}). ^{13}C NMR (126 MHz, DMSO-d6) δ 167.40 , 151.82 , 150.72 , 150.26 , 147.17 , 146.54 , 145.39 , 145.06 , 144.61 , 141.26 , 139.12 , 139.06 , 136.39 , 136.17 , 132.84 , 132.37 , 131.75 , 131.46 , 130.55 , 130.16 , 129.98 , 129.37 , 128.37 , 127.89 , 127.15 , 126.65 , 125.45 , 125.18 , 124.34 , 124.19 , 122.93 , 122.82 , 120.88 , 120.10 , 113.68 , 18.36. ESI-MS m/z: Calculated ms: 836.21, found:836.30 $[M\text{-}PF_6]^+$. Elemental analysis calcd (%) for $C_{46}H_{37}F_6IrN_7P$: C 53.90, H 3.64, and N 9.57; found: C 53.88, H 3.69, and N 9.53.

Data for **PytMP-Ir**: IR (KBr): 3661, 3042, 2929, 2366, 2028, 1587, 1568, 1540, 1475, 1427, 1334, 1268, 1109, 1051, 846, 752, 546. ^{1}H NMR (500 MHz, DMSO-d_6) δ 9.61 (s, 1H, H_9), 9.28 (s, 1H, H_{16}), 8.30 (dd, J = 17.2, 8.2 Hz, 2H, H_{10}, and H_{11}), 8.23 – 8.08 (m, 2H, H_1 and $H_{1'}$), 7.95 (ddd, J = 47.6, 22.5, 7.6 Hz, 6H, H_4, $H_{4'}$, H_5, $H_{5'}$, H_{12} and H_{15}), 7.62 (d, J = 9.3 Hz, 3H, H_6, $H_{6'}$, and H_{19}), 7.21 – 6.89 (m, 6H, H_3, $H_{3'}$,H_7, H_7',H_8, and $H_{8'}$), 6.45 (d, J = 7.5 Hz, 2H, H_2 and $H_{2'}$), 6.23 (d, J = 9.2 Hz, 1H, H_{18}), 2.51 (s, 3H, H_{13}), 2.50 (s, 3H, H_{14}), 2.43 (s, 3H, H_{17}). ^{13}C NMR (126 MHz, DMSO-d6) δ 167.78, 167.37, 151.56, 150.57, 147.59, 146.71, 145.58, 145.44, 145.02, 143.63, 141.70, 139.49, 139.35, 136.11, 132.48, 131.75, 130.61, 130.25, 127.23, 127.03, 126.06, 125.53, 125.29, 124.56, 124.23, 123.11, 122.95, 119.9 , 113.64, 20.55, 20.38, 18.36. ESI-MS m/z: Calculated ms: 864.24, found: 864.50 $[M\text{-}PF_6]^+$. Elemental analysis calcd (%) for $C_{48}H_{41}F_6IrN_7P$: C 54.75, H 3.92, and N 9.31; found: C 54.73, H 3.93, and N 9.29.

Data for **MPyP-Ir**: IR (KBr):3661, 3042, 2920, 2853, 2356, 1728, 1634, 1478, 1456, 1450, 1418, 1334, 1268, 1109, 1034, 837, 743, 556. ^{1}H NMR (500 MHz, DMSO-d_6) δ 10.13 (t, J = 7.7 Hz, 1H, H_9), 9.65 (d, J = 8.1 Hz, 1H, H_{16}), 8.53 (dd, J = 23.8, 8.4 Hz, 2H, H_1 and $H_{1'}$), 8.20 (t, J = 7.6 Hz, 1H, H_{11}), 8.16 – 8.00 (m, 5H, H_{12}, H_{15}, H_5, $H_{5'}$ and H_{13}), 7.95 (d, J = 5.4 Hz, 1H, H_{14}), 7.82 – 7.67 (m, 4H, H_3, $H_{3'}$,H_6 and $H_{6'}$), 7.63 (t, J = 6.8 Hz, 1H, H_{10}), 7.14 (dt, J = 33.2, 7.7 Hz, 2H, H_7 and $H_{7'}$), 7.04 – 6.92 (m, 3H, H_8, $H_{8'}$ and H_{19}), 6.90 – 6.83 (m, 1H, H_{18}), 6.43 (d, J = 7.5 Hz, 1H, H_{17}), 6.27 (dd, J = 54.0, 8.3 Hz, 2H, H_2 and $H_{2'}$), 2.83 (s, 3H, H_4), 2.80 (s, 3H, $H_{4'}$). ^{13}C NMR (126 MHz, DMSO-d6) δ 165.24, 165.04, 149.48, 149.13, 148.65, 148.09, 146.89, 146.83, 144.48, 142.73, 141.24, 139.97, 137.01, 136.07, 133.51, 133.00, 132.66, 132.64, 132.41, 131.66, 131.53, 131.09, 130.01, 129.59, 129.18, 128.98, 128.64, 127.99, 127.21, 123.63, 123.47, 122.60, 122.52, 121.18, 116.61, 114.44, 23.06, 22.98. ESI-MS m/z: Calculated ms: 850.22, found:850.50 $[M\text{-}PF_6]^+$. Elemental analysis

calcd (%) for $C_{47}H_{38}F_6IrN_7P$: C 54.38, H 3.69, and N 9.45; found: C 54.35, H 3.71, and N 9.44.

Data for **MPydMP-Ir**: IR (KBr):3670, 3051, 2910, 2356, 1606, 1540, 1425, 1409, 1315, 1259, 1105, 1099, 1043, 1015, 837, 771, 566. ^{1}H NMR (500 MHz, Chloroform-*d*) δ 10.14 (d, *J* = 6.4 Hz, 1H, H_9), 9.64 (d, *J* = 8.1 Hz, 1H, H_{16}), 8.21 (s, 1H, H_{11}), 8.09 (s, 1H, H_{10}), 8.05 – 7.99 (m, 3H, H_{12}, H_1 and $H_{1'}$), 7.87 – 7.79 (m, 2H, H_5 and $H_{5'}$), 7.62 (d, *J* = 5.2 Hz, 1H, H_{15}), 7.54 – 7.41 (m, 4H, H_3, $H_{3'}$, H_6 and $H_{6'}$), 7.13 (dt, *J* = 25.7, 7.6 Hz, 2H, H_7 and $H_{7'}$), 6.97 (dt, *J* = 15.8, 7.3 Hz, 2H, H_8 and $H_{8'}$), 6.83 (dt, *J* = 23.4, 6.3 Hz, 2H, H_2 and $H_{2'}$), 6.54 (d, *J* = 7.5 Hz, 1H, H_{19}), 6.45 (d, *J* = 7.4 Hz, 1H, H_{18}), 6.26 (d, *J* = 8.9 Hz, 1H, H_{17}), 2.85 (s, 3H, H_4), 2.82 (s, 3H, $H_{4'}$), 2.62 (s, 3H, H_{13}), 2.59 (s, 3H, H_{14}). ^{13}C NMR (126 MHz, DMSO-d6) δ 164.98, 151.34, 149.37, 148.94, 147.68, 146.95, 146.50, 145.45, 143.86, 142.95, 142.80, 139.10, 138.48, 135.57, 133.28, 132.92, 132.62, 132.56, 131.75, 130.41, 129.58, 129.25, 129.03, 128.71, 127.49, 127.34, 127.21, 123.94, 123.43, 122.74, 122.56, 120.53, 116.03, 114.37, 23.14, 23.08, 20.64, 20.38. ESI-MS m/z: Calculated ms: 878.11, found:878.80 $[M\text{-}PF_6]^+$. Elemental analysis calcd (%) for $C_{49}H_{43}F_6IrN_7P$: C 55.15, H 4.06, and N 9.19; found: C 55.12, H 4.10, and N 9.16.

Data for **MPyMP-Ir**: IR (KBr): 3679, 3061, 2910, 2356, 1728, 1587, 1540, 1427, 1521, 1324, 1250, 1099, 1024, 846, 752, 556. ^{1}H NMR (500 MHz, DMSO-d_6) δ 9.90 (s, 1H, H_9), 9.62 (d, *J* = 8.1 Hz, 1H, H_{16}), 8.61 (d, *J* = 8.5 Hz, 1H, H_{11}), 8.48 (d, *J* = 8.4 Hz, 1H, H_{10}), 8.22 – 8.02 (m, 6H, H_1, $H_{1'}$, H_5, $H_{5'}$, H_6 and $H_{6'}$), 7.93 (d, *J* = 5.6 Hz, 1H, H_{12}), 7.76 (dd, *J* = 23.5, 6.6 Hz, 3H, H_{15}, H_3, and $H_{3'}$), 7.65 – 7.59 (m, 1H, H_{13}), 7.13 (dt, *J* = 30.6, 7.7 Hz, 2H, H_7 and $H_{7'}$), 7.03 – 6.94 (m, 3H, H_{14}, H_8 and $H_{8'}$), 6.87 (dd, *J* = 7.5, 6.0 Hz, 1H, H_{19}), 6.37 (dd, *J* = 42.1, 7.5 Hz, 2H, H_2, and $H_{2'}$), 6.12 (d, *J* = 9.3 Hz, 1H, H_{18}), 2.83 (s, 3H, H_4), 2.79 (s, 3H, $H_{4'}$), 2.54 (s, 3H, H_{17}). ^{13}C NMR (126 MHz, DMSO-d6) δ 165.20, 165.06, 151.43, 149.07, 148.61, 146.96, 146.89, 146.54, 144.36, 142.81, 142.70, 141.24, 137.05, 136.29, 136.05, 132.83, 132.64, 132.38, 131.68, 131.46, 129.9 , 129.57, 129.3 , 129.14, 128.98, 128.62, 128.33, 127.09, 126.64, 123.62, 123.46, 122.56, 120.86, 113.70, 23.05, 22.98, 18.34. ESI-MS m/z: Calculated ms: 864.24, found: 864.50 $[M\text{-}PF_6]^+$. Elemental analysis calcd (%) for $C_{48}H_{41}F_6IrN_7P$: C 54.75, H 3.92, and N 9.31; found: C 54.72, H 3.95, and N 9.28.

Data for **MPytMP-Ir**: IR (KBr): 3661, 3051, 2929, 2366, 1625, 1578, 1540, 1475, 1339, 1334, 1296, 1270, 1109, 1024, 837, 724, 565. ^{1}H NMR (500 MHz, DMSO-d_6) δ 9.50 (s, 1H), 9.14 (s, 1H), 8.18 – 7.90 (m, 6H), 7.83 (s, 2H), 7.72 (d, *J* = 7.6 Hz, 1H), 7.59 (d, *J* = 9.4 Hz, 1H), 7.16 (dt, *J* = 37.3, 7.7 Hz, 4H), 7.00 (dt, *J* = 10.9, 7.4 Hz, 2H, H_8 and $H_{8'}$), 6.88 – 6.83 (m, 1H, H_{19}), 6.41 (dd, *J* = 12.8, 7.5 Hz, 2H, H_2 and $H_{2'}$), 6.05 (d, *J* = 9.1 Hz, 1H, H_{18}), 2.85 (s, 3H, H_4), 2.83 (s, 3H, $H_{4'}$), 2.51 (s, 3H, H_{13}), 2.46 (s, 3H, H_{14}), 2.32 (s, 3H, H_{17}). ^{13}C NMR (126 MHz, DMSO-d_6) δ 165.57, 165.05, 149.34, 148.87, 146.96, 146.90, 146.45, 145.35, 143.49, 143.37, 143.10, 142.86, 139.36, 138.61, 138.14, 135.99, 133.06, 132.71, 132.54, 131.69, 129.63, 129.27, 129.07, 128.76, 127.08, 126.82, 125.93, 123.46, 122.76, 122.62, 119.88, 113.68, 23.20, 23.09, 20.52, 20.32, 18.32. ESI-MS m/z: Calculated ms: 892.27, found: 892.70 $[M\text{-}PF_6]^+$. Elemental analysis calcd (%) for $C_{50}H_{45}F_6IrN_7P$: C 55.55, H 4.20, and N 9.07; found: C 55.54, H 4.23, and N 9.08.

The other experimental methods

MTT assay

The synthesized compounds (2.0 mM) were prepared as DMSO stock solutions and Tris-HCl buffer solution (10 mM, pH 7.35), and the stock solutions were stored at 4.0 °C for no more than 6.0 d before use. The final DMSO in the working solution was limited to 5 % in all the assays.

The cell culture was maintained on RPMI-1640 medium supplemented with 10% fetal bovine serum, 100 U/mL penicillin and 100 μg/mL streptomycin in 25 cm^2 culture flasks at 37 °C humidified atmosphere with 5% CO_2. All different cells to be tested in the following assays have a passage number of 3−6.

The cells 5.0×10^3 per well were seeded in triplicate in 96-well plates and incubated for 24 h at 37 °C and 5% CO_2/95% air. Then graded amounts of compound were added to the wells in 10 μL of PBS free culture medium and the plates were incubated in a 5% CO_2 humidified atmosphere for 48 h. Six replica wells were used as controls. Cells were grew for 12 h before treatment to reach 70% confluency and 20 μL of tested various concentrations of compounds were added to each well. The final concentration of the tested pyrido [3,2-a] pyrido [1',2':1,2] imidazo [4,5-c] phenazine (**P**), 12,13-dimethyl pyrido [3,2-a] pyrido [1',2':1,2] imidazo [4,5-c] phenazine (**dMP**), 2-methylpyrido [3,2-a] pyrido [1',2':1,2] imidazo [4,5-c] phenazine (**MP**) and 2,12,13-trimethylpyrido [3,2-a] pyrido [1',2':1,2] imidazo [4,5-c] phenazine (**tMP**), **MPytMP-Ir, MPydMP-Ir, PytMP-Ir, PydMP-Ir, MPyMP-Ir, PyMP-Ir, MPyP-Ir** and **PyP-Ir** were kept at 1.0 nM, 10 nM, 100nM, 500nM, 1.0μM, 1.25μM, 2.5μM, 5μM, 10μM, 20 μM, respectively. After 48 h of culture, 0.1 mg of MTT (in 20 μL of PBS) was added to each well, and cells were incubated at 37 °C for 6 h. The formed formazan crystals were then dissolved in 100 μL of DMSO and the absorbance was read by enzyme labeling instrument with 490/630 nm double wavelength measurement. The final IC_{50} values of **MPytMP-Ir, MPydMP-Ir, PytMP-Ir, PydMP-Ir, MPyMP-Ir, PyMP-Ir, MPyP-Ir** and **PyP-Ir** were calculated by the Bliss method (n = 5). All tests were repeated in at least 3.0 independent trials.

TRAP-silver staining assay

Telomerase extract was prepared from NCI-H460 tumor cells. A modified version of the TRAP assay was used. PCR was performed in a final 50 μL reaction volume composed of reaction mix (45 μL) containing Tris-HCl (20 mM, pH 8.0), deoxynucleotide triphosphates (50 mM), $MgCl_2$ (1.5 mM), KCl (63 mM), EGTA (1 mM), Tween-20 (0.005%), BSA (20.0 μg/mL), primer HTG21 (3.5 pmol; 5'-G_3ACHTUNGTRENUNG[T_2AG_3]3-3'), primer TS (18 pmol; 5'-AATCCG TCGAGCAGAGTT-3'), primer CXext (22.5 pmol; 5'-GTGCCCTTACCCTT ACCCTTACCCTAA-3'), primer NT (7.5 pmol; 5'-ATCGCTTCTCGGCCTTTT-3'), TSNT internal control (0.01 amol; 5'-ATTCCGTCGAGCAGAGTTAAAAGG CCGAGAAGCGAT-3'), Taq DNA polymerase (2.5 U), and telomerase (100 ng). **MPydMP-Ir** (125 nM) and **MPytMP-Ir** (5 nM) or distilled water were added (5 μL). PCR was performed in an Eppendorf Master cycler equipped with a hot lid and incubated for 30 min at 30 °C, followed by 92 °C 30 s, 52 °C 30 s, and 72 °C 30 s for 30 cycles. After amplification, loading buffer (8 μL; 5×TBE buffer, 0.2% bromophenol blue, and 0.2% xylene cyanol) was added to the reaction. An aliquot (15.0 μL) was loaded onto a nondenaturing acrylamide gel (16%; 19:1) in 1×TBE buffer and resolved at 200.0 V for 1.0 h. The Gels were fixed and then stained with 5-10% $AgNO_3$.

Cell Cycle

In cell cycle analysis, the NCI-H460 tumor cells were maintained with 10% fetal calf serum in 5% CO_2 at 37°C. After treated with

MPydMP-Ir (125 nM) and **MPytMP-Ir** (5 nM) for 24.0 h, the cells were harvested by trypsinization and rinsed with PBS. After centrifugation, the pellet (10^5−10^6 cells) was suspended in 1.0 mL of PBS and then fixed by dropwise addition of 9 mL of precooled (4 °C) 70% ethanol under violent shaking. After treatment, cells were collected and fixed with ice-cold 70% ethanol at −20 °C overnight. Fixed cells were resuspended in 0.5 mL of PBS containing 50 μg/mL propidium iodide and 100 μg/mL RNase A. The cell cycle distribution was analyzed by FACS Calibur flow cytometer (BD) and calculated using ModFIT LT software (BD).

Cell apoptosis

The cell apoptosis was detected by flow cytometric analysis of annexin V staining. After treated with **MPydMP-Ir** (125 nM) and **MPytMP-Ir** (5 nM) for 24.0 h, the cells were harvested by trypsinization and rinsed with PBS. Briefly, adherent NCI-H460 tumor cells were harvested and suspended in the annexin-binding buffer (5×10^5 cells/mL). Then cells were incubated with annexin V-FITC and PI for 1.5 h at room temperature in the dark and immediately analyzed by flow cytometry. The data are presented as biparametric dot plots showing PI red fluorescence vs annexin V-FITC green fluorescence.

Flow cytometry analysis of mitochondrial membrane potential (MMP, ΔΨm)

JC-1 Assay Kit was used to detect the changes of MMP. The NCI-H460 tumor cells (5×10^5 cells/mL) were inoculated in 6-well plate for 24 h and then treated with **MPydMP-Ir** (125 nM) and **MPytMP-Ir** (5 nM) for 24 h. After incubation, the NCI-H460 tumor cells were washed and resuspended with PBS. For analysis, 0.5 mL PBS buffer solution (lincluding 10 μg/mL JC-1 staining) was added into the suspension in darkness for 30.0 min at 37 ° C. The green fluorescence percentage from JC-1 monomers was detected by flow cytometry, which demonstrated the decrease of MMP.

Western blotting

The NCI-H460 tumor cells harvested from each well of the culture plates were lysed in 150 μL of extraction buffer consisting of 149 μL of RIPA Lysis Buffer and 1 μL PMSF (100 mM). The suspension was centrifuged at 10000 rpm at 4 °C for 10 min, and the supernatant (10 μL for each sample) was loaded onto 10% polyacrylamide gel and then transferred to a microporous polyvinylidene difluoride (PVDF) membrane. Western blotting was performed using each target antibody and horseradish peroxidase-conjugated antimouse or antirabbit secondary antibody. Protein bands were visualized using chemiluminescence substrate.

Acute Toxicity Studies

The NCI-H460 xenograft mouse models were purchased from Beijing HFK Bioscience Co., Ltd (Beijing, China, approval No. SCXK 2014-004). The animal procedures were approved by the Institute of Radiation Medicine Chinese Academy of Medical Sciences (Tian Jin, China, approval No. SYXK 2014-0002). And all of the experimental procedures were carried out in accordance with the NIH Guidelines for the Care and Use of Laboratory Animals. Animal experiments were approved by the Animal Care and Use Committee of Institute of Radiation Medicine Chinese Academy of Medical Sciences. In addition, six-week old male and female KM mice (weight 20−22 g) were randomly divided into 3 groups (n = 6) and used to study the in vivo safety of **MPytMP-Ir**. The highest solubility of **MPytMP-Ir** in solvent (5% v/v DMSO/saline) was used as the solution, and a good practice volume (0.6 mL/20 g) by intraperitoneal injection was used. The group of KM mice were treated with **MPytMP-Ir** at dose 10.0 mg/kg every two day (5% v/v DMSO/saline), respectively, and one group received the same volume of solvent and used as the control. The signs of toxicity were observed, and body

weight was recorded daily. The highest soluble **MPytMP-Ir** (10.0 mg/kg) in solvent (5% v/v DMSO/saline) was used as the solution to conduct preliminary study on its safety, and the ICR mice received a possible maximal administration[1] values (1.0 mL/20.0 g) by intraperitoneal injection. The solubility of **MPytMP-Ir** was over 0.2 mg/mL in in solvent (5% v/v DMSO/saline) at room temperature.

Anti-cancer activity toward NCI-H460 cancer xenograft in vivo

The NCI-H460 cells were harvested and injected subcutaneously into the right flank of nude mice with 5×10^6 cells in 200 μL of serum-free medium. When the xenograft tumor growth to the volume about 1000 mm^3, the mice were killed and the tumor tissue were cut into about 1.5 mm^3 small pieces, and then transplanted into the right flank of female nude mice, When tumors reach a volume of 100-400 mm^3 on all mice, the mice were randomized into vehicle control and treatment groups (n=6/group), received the following treatments: (a) control, 5% v/v DMSO/saline vehicle, (b) **MPytMP-Ir** at dose 10.0 mg/kg every two day (5% v/v DMSO/saline). The tumor volumes were determined every three days by measuring length (*l*) and width (*w*) and calculating volume, tumor volume and inhibition of tumor growth were calculated using formulas [1–17]:

Tumor volume: $V = (w^2\times l)/2$ (1)

The tumor relative increment rate: $T/C\ (\%) = T_{RTV}/C_{RTV}\times100\%$ (2)

inhibition of tumor growth: $IR(\%) = (W_c - W_t)/W_c\times100\%$ (3)

Where w and l mean the shorter and the longer diameter of the tumor respectively; T_{RTV} and C_{RTV} was the RTV of treated group and control group respectively. (RTV: relative tumor volume, $RTV= V_t /V_0$); W_t and W_c mean the average tumor weight of complex-treated and vehicle controlled group respectively.

Statistical Analysis

The experiments have been repeated from three to five times, and the results obtained are presented as means ± standard deviation (SD). Significant changes were assesses by using Student's *t* test for unpaired data, and p values of <0.05 were considered significant.

Abbreviations

SD, standard deviation; TBS, Tris-HCl buffer; MTT, 3-(4,5-dimethylthiazol-2-yl)-2,5-diphenyltetrazolium bromide; TGI, tumor growth inhibition; PI, propidium iodide; MMP, mitochondrial membrane potential; JC-1, 5,5′,6,6′-tetrachloro-1,1′,3,3′-tetraethylbenzimidazolylcarbocyanine; IR, tumor growth inhibition rate.

Results

The in Vivo Antitumor Activity toward NCI-H460 by MPytMP-Ir.

The antitumor models of NCI-H460 was applied to study the inhibition activity of tumor growth of **MPytMP-Ir**. The moment that the tumor volume had grown to around 200-400 mm^3, the NCI-H460 xenograft mice were randomizingly putted into control and treating mice with a single intraperitoneously injection of **MPytMP-Ir** at a dose of 10.0 mg/kg to measure and record the mortality rate of mice induced by control and **MPytMP-Ir** over 12 days. We observed the mouse for 24 h for collecting the indication of toxicity and mortality. As shown in Figure 5A and Table S2, we could clearly find that the average tumor volumes of the **MPytMP-Ir** group grew slowly with an average volume of 600.62±157.03 mm^3, corresponding to relative tumor increment rates of 38.2% while the control group grew

rapidly and reached up to average volume of 1544.41 ± 225.83 mm^3 on day 12.0. We killed the mice to collect and record the values of tumor weight and count inhibition rate of tumor growth according to the tumor weight on Day 12. As we can see in Figure 5B and Table S3, inhibition rate of tumor growth of **MPytMP-Ir** was 47.1%, significantly higher than that of cisplatin (25.5%) to some extent.[1-17] Comparing with the control groups, the mouse in **MPytMP-Ir** treatment group behaved healthy without any visible signs of abnormality and their body weights kept increasing (Figure 5C and Tables S2-S4). The average body weight of treating mice with a single intraperitoneously injection of **MPytMP-Ir** at a dose of 10.0 mg/kg increasing from 18.47 ± 1.08 to 20.37 ± 0.52 g, while the control group increasing from 18.03 ± 1.28 to 20.28 ± 0.47g. In summary, all the results demonstrated that **MPytMP-Ir** effectively displayed inhibition of tumor growth in NCI-H460 models. Furthermore, **MPytMP-Ir** exhibited less toxicity even better safety profile than that of cisplatin.

■ REFERENCES

(1) (a) Leung, K.-H.; He, H.-Z.; He, B.; Zhong, H.-J.; Lin, S.; Wang, Y.-T.; Ma, D.-L.; Leung, C.-H. Label-free luminescence switch-on detection of hepatitis C virus NS3 helicase activity using a G-quadruplex-selective probe. *Chem. Sci.* **2015**, *6*, 2166–2171. (b) Chen, Z. F.; Qin, Q. P.; Qin, J. L.; Zhou, J.; Li, Y. L.; Li, N.; Liu, Y. C.; Liang, H. Water-soluble ruthenium(II) complexes with chiral 4-(2,3-dihydroxypropyl)-formamide oxoaporphine (FOA): in vitro and in vivo anti-cancer activity by stabilization of G-Quadruplex DNA, inhibition of telomer-ase activity, and induction of tumor cell apoptosis. J. Med. Chem. 2015, 58, 4771−4789.

(2) Cao, R.; Jia, J.-L.; Ma, X.-C.; Zhou, M.; Fei, H. Membrane localized iridium(III) complex induces endoplasmic reticulum stress and mitochondria-mediated apoptosis in human cancer cells. *J. Med. Chem.* **2013**, *56*, 3636−3644.

(3) Palanimuthu, D.; Shinde, S. V.; Somasundaram, K.; Samuelson, A. G. In vitro and in vivo anticancer activity of copper bis(thiosemicarbazone) complexes, *J. Med. Chem.* **2013**, *56*, 722–734.

(4) Wilson, J. J.; Lippard, S. J. In vitro anticancer activity of cis-diammineplatinum(II) complexes with β-diketonate leaving group ligands. *J. Med. Chem.* **2012**, *55*, 5326−5336.

(5) Kassab, A. E.; Gedawy, E. M. Novel ciprofloxacin hybrids using biology oriented drug synthesis (BIODS) approach: Anticancer activity, effects on cell cycle profile, caspase-3 mediated apoptosis, topoisomerase II inhibition, and antibacterial activity. *Eur. J. Med. Chem.* **2018**, *150*, 403−418.

(6) Liu, F.; Gou, S.; Chen, F.; Fang, L.; Zhao, J. Study on antitumor platinum(II) complexes of chiral diamines with dicyclic species as steric hindrance. *J. Med. Chem.* **2015**, *58*, 6368−6377.

(7) Qin, Q.-P.; Wang, S.-L.; Tan, M.-X.; Wang, Z.-F.; Luo, D.-M.; Zou, B.-Q.; Liu, Y.-C.; Yao, P.-F.; Liang, H. Novel tacrine platinum(II) complexes display high anticancer activity via inhibition of telomerase activity, dysfunction of mitochondria, and activation

of the p53 signaling pathway. *Eur. J. Med. Chem*. **2018**, *158*, 106−122.

(9) Sheldrick, G. M. SHELXTL-97, Program for refinement of crystal structures, University of Göttingen, Germany, 1997.

(9) Qian, C.; Wang, J.-Q.; Song, C.-L.; Wang, L.-L.; Ji, L.-N.; Chao, H. The induction of mitochondria-mediated apoptosis in cancer cells by ruthenium(II) asymmetric complexes. Metallomics 2013, 5, 844−854.

(10) Aird, R. E.; Cummings, J.; Ritchie, A. A.; Muir, M.; Morris, R. E.; Chen, H.; Sadler, P. J.; Jordrell, D. I. In vitro and in vivo activity and cross resistance profiles of novel ruthenium(II) organometallic arene complexes in human ovarian cancer. Br. J. Cancer 2002, 86, 1652−1657.

(11) Chen, Z.-F.; Qin, Q.-P.; Qin, J.-L.; Liu, Y.-C.; Huang, K.-B.; Li, Y.-L.; Meng, T.; Zhang, G.-H.; Peng, Y.; Luo, X.-J.; Liang, H. Stabilization of G-quadruplex DNA, inhibition of telomerase activity and tumor cell apoptosis of organoplatinum(II) complexes with oxoisoaporphine. J. Med. Chem. 2015, 58, 2159−2179.

(12) Yi, Q. Y.; Wan, D.; Tang, B.; Wang, Y. J.; Zhang, W. Y.; Du, F.; He, M.; Liu, Y. J. Synthesis, characterization and anticancer activity in vitro and in vivo evaluation of an iridium(III) polypyridyl complex. *Eur. J. Med. Chem*. **2018**, *145*, 338-349.

(13) Qin, Q. P.; Wang, Z. F.; Wang, S. L.; Luo, D. M.; Zou, B. Q.; Yao, P. F.; Tan, M. X.; Liang, H. In vitro and in vivo antitumor activities of three novel binuclear platinum(II) complexes with 4′-substituted-2, 2′: 6′, 2 ″-terpyridine ligands. *Eur. J. Med. Chem.* **2019**, *170*, 195-202.

(14) Meng, T.; Qin, Q. P.; Chen, Z. L.; Zou, H. H.; Wang, K.; Liang, F. P. High in vitro and in vivo antitumor activities of Ln(III) complexes with mixed 5,7-dichloro-2-methyl-8-quinolinol and 4,4′-dimethyl-2,2′-bipyridyl chelating ligands. *Eur. J. Med. Chem.* **2019**, *169*, 103-110.

(15) Huang, G. B.; Chen, S.; Qin, Q. P.; Luo, J. R.; Tan, M. X.; Wang, Z. F.; Zou, B. Q.; Liang, H. In vitro and in vivo activity of novel platinum(II) complexes with naphthalene imide derivatives inhibiting human non-small cell lung cancer cells. *New J. Chem.* **2019**, *43*, 8146-8152.

(16) Qin, Q. P.; Wang, Z. F.; Huang, X. L.; Tan, M. X.; Shi, B. B.; Liang, H. High in Vitro and in Vivo Tumor-Selective Novel Ruthenium(II) Complexes with 3‑(2′-Benzimidazolyl)-7-fluoro-coumarin. *ACS Med. Chem. Lett.* **2019**, *10*, 936-940.

(17) Messori, L.; Casini, A.; Gabbiani, C.; Michelucci, E.; Cubo, L.; Ríos-Luci, C.; Padrón, J. M.; Navarro-Ranninger, C.; Quiroga, A. G. Cytotoxic profile and peculiar reactivity with biomolecules of a novel “rule-breaker” iodidoplatinum(II) complex. *ACS Med. Chem. Lett.* **2010**, *1*, 381–385.

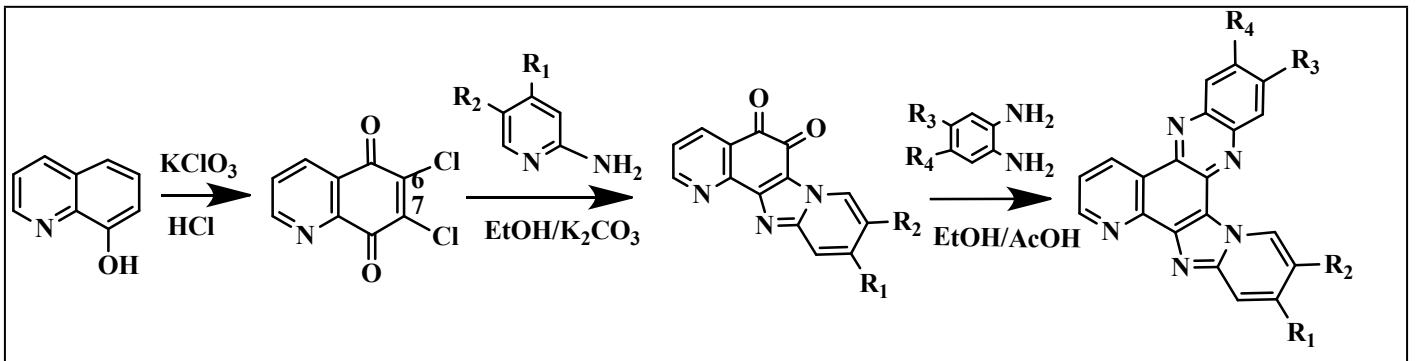

Chart S1. Synthesis of the main ligand in this work.

Table S1. IC_{50} values (μM) of eight Ir(III) complexes and five the corresponding ligand against four human cell lines [a]. [a] IC_{50} values are presented as mean ± SD (standard error of the mean) from five independent experiments. The cells were incubated with each compound for 48 h. [b] The stock solution of cisplatin was prepared at a concentration of 1.0 mM with 0.154 M NaCl. [c] The concentration unit was nM.

	NCI-H460	T-24	HeLa	HL-7702
H-Py	>150	>150	>150	>100
P	67.06±1.25	>100	60.11±0.23	70.26±0.59
dMP	60.02±1.84	72.01±1.73	52.03±0.49	65.03±1.05
MP	54.21±0.59	61.52±2.06	48.64±1.15	62.03±1.56
tMP	49.36±1.22	55.05±1.34	30.89±0.74	60.23±0.67
H-MPy	>150	>100	>100	>100
MPytMP-Ir	5.05±0.22 nM [c]	1.07±0.36	1.88±0.21	63.02±1.98
MPydMP-Ir	125.26±0.56 nM [c]	4.58±0.79	3.90±0.45	57.03±0.48
PytMP-Ir	520.00±0.95 nM [c]	6.01±1.05	5.00±0.69	55.02±1.06
PydMP-Ir	1.09±1.02	9.95±0.55	6.06±1.14	52.03±1.17
MPyMP-Ir	2.81±1.02	11.93±1.63	10.41±184	56.72±1.85
PyMP-Ir	2.52±0.71	20.23±1.09	12.17±0.19	50.12±0.47
MPyP-Ir	4.53±0.86	25.11±1.12	12.93±0.78	60.25±1.06
PyP-Ir	6.61±0.93	31.28±0.78	24.46±1.54	65.21±1.85

cisplatin [b]		11.15±0.35	15.06±1.85	13.01±1.15	15.06±1.12

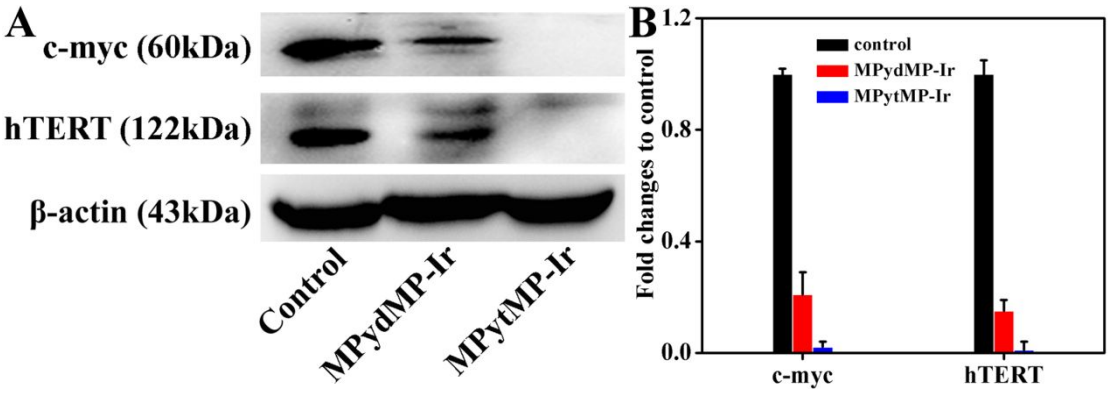

Figure S1. The treatment of c-myc and hTERTE expression in the NCI-H460 tumor cells treated with with **MPydMP-Ir** (125 nM) and **MPytMP-Ir** (5 nM) for 24 h by Western blot. (A) Western blot images. (B) column density indication of the express levels of c-myc and hTERT.

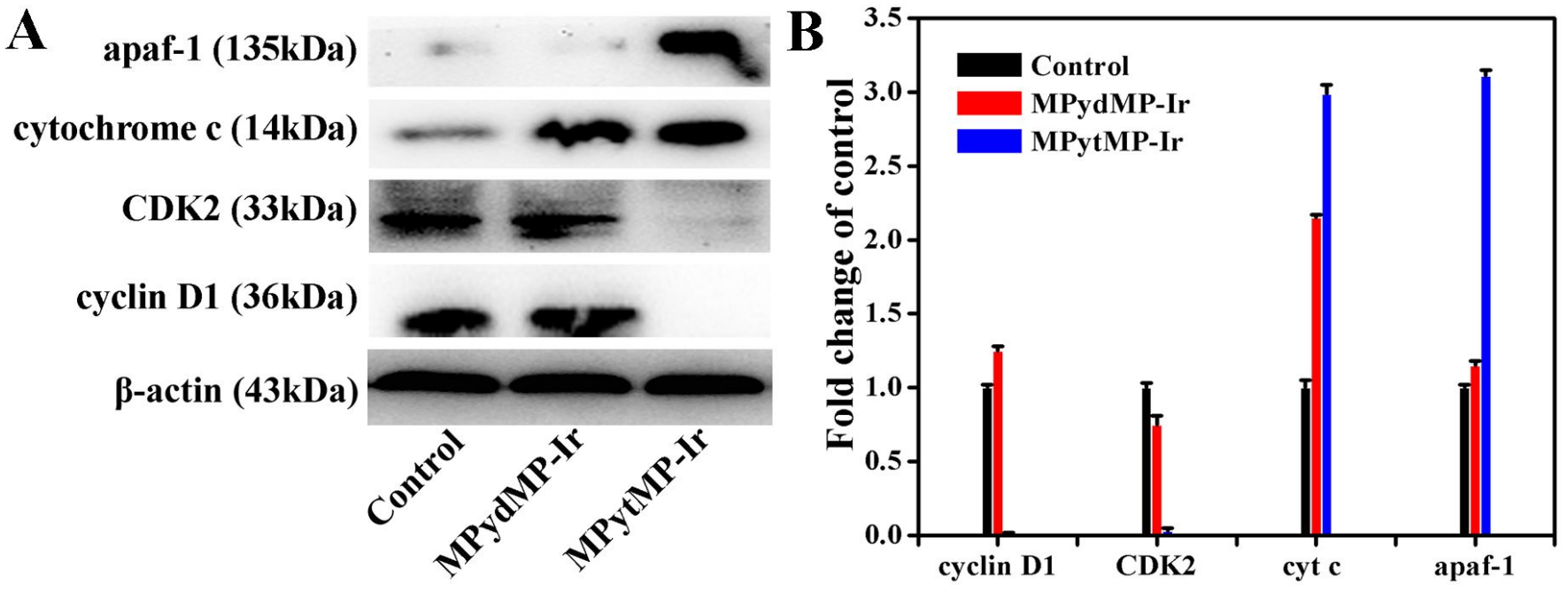

Figure S2. G1-phase and apoptosis related proteins(A) the the express levels of G1-phase related proteins CDK2 and Cyclin D1(bottom two) and apoptosis related proteins apf-1 and cytochrome c (top two) in NCI-H460 cells treated with **MPydMP-Ir**(125 nM) and **MPytMP-Ir**(5 nM) for 24 h were examined by Western blotting. (B) the analysis on Western blot using antibodies against G1-phase(left) and apoptosis (right) related proteins.

Table S2. The tumor volume in treated and non-treated mice from the date of surgery to the study end point in the NCI-H460 xenograft model.

Group		**Tumor Volume (mm^3)**		**T/C**
		(start)	**(end)**	**(%)**
Control		72.42±12.94	1544.41±225.83	-
MPytMP-Ir	(10.0	72.90±8.81	600.62±157.03	38.2[a]

mg/kg)

[a] mean $p<0.05$, *p vs* vehicle control

Table S3. In Vivo Anticancer Activity of each complex toward NCI-H460 Tumor Xenograft.

Group	**average tumor weight(mean ± SD g)**	**inhibition of tumor growth(%)**
Control	1.56±0.14	-
MPytMP-Ir (10.0 mg/kg)	0.82±0.22	47.1[a]

[a] mean $p<0.05$, *p vs* control.

Table S4. Average body weight in treated and non-treated mice from the date of surgery to the study end point in the NCI-H460 xenogfart model.

Group	**Body Weight (g)**		**RBW (%)**
	(start)	**(end)**	**(end)**
Control	18.03±1.28	20.28±0.47	112.48
MPytMP-Ir (10.0 mg/kg)	18.47±1.08	20.37±0.52	110.29

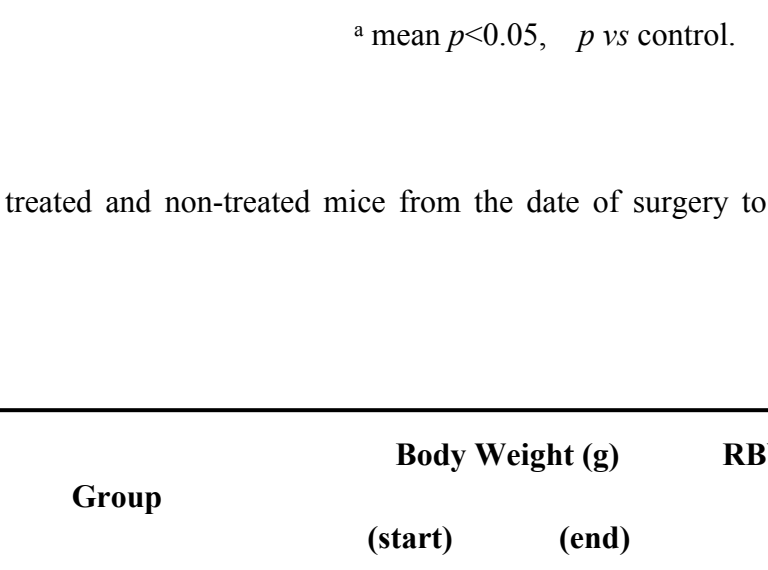

Figure S3. IR (KBr) spectra of **P**.

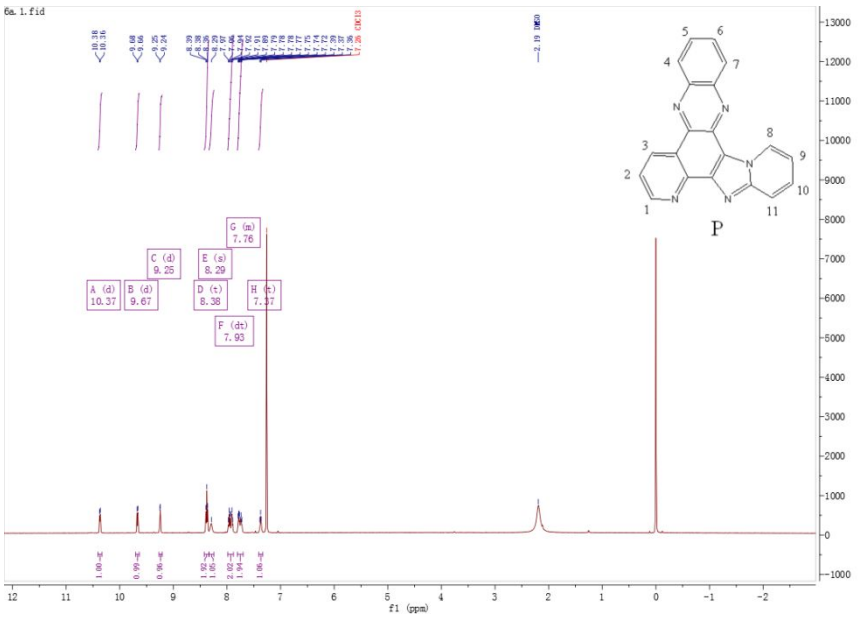

Figure S4. [1]H NMR (500 MHz, Chloroform-d) for **P**.

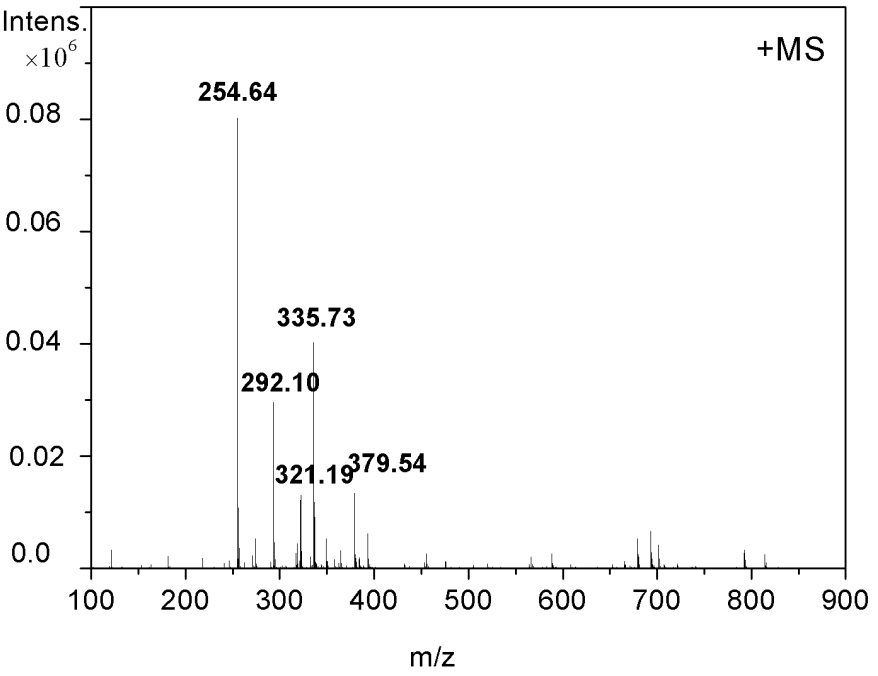

Figure S5. The mass spectra of **P** in DMSO for 0 h .

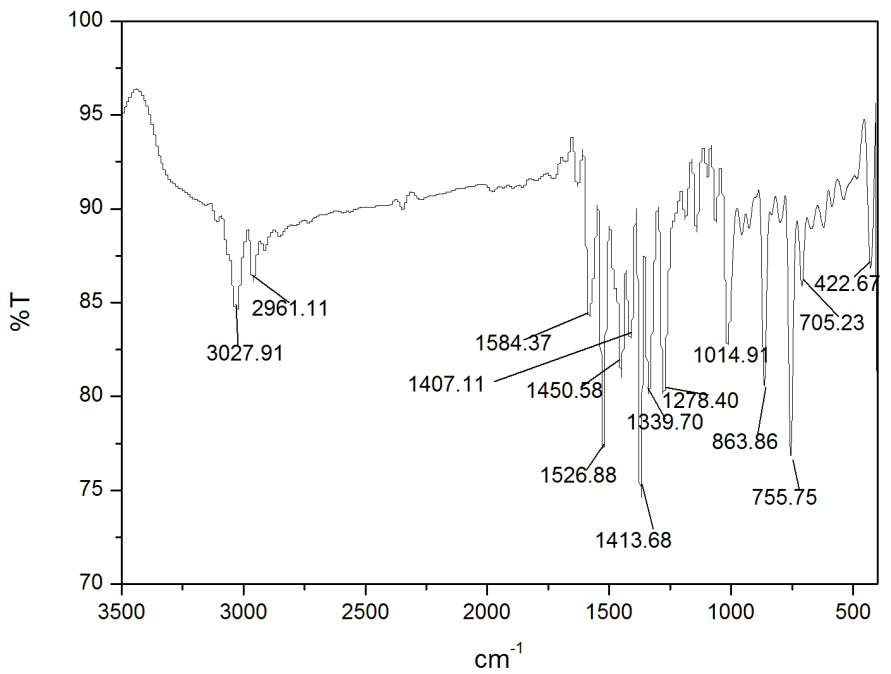

Figure S6. IR (KBr) spectra of **dMP**.

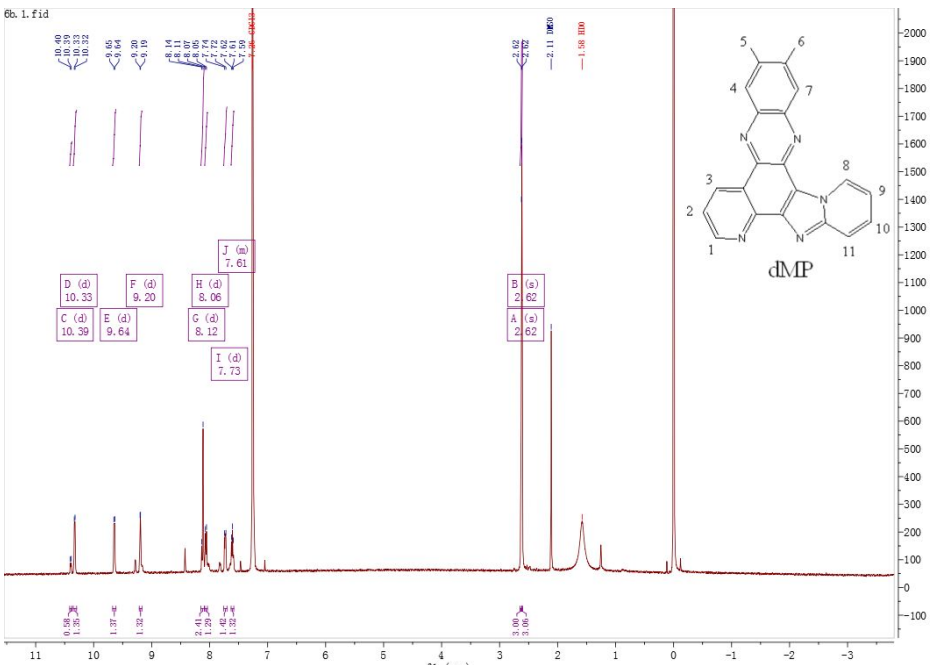

Figure S7. ^{1}H NMR (500 MHz, Chloroform-d) for **dMP**

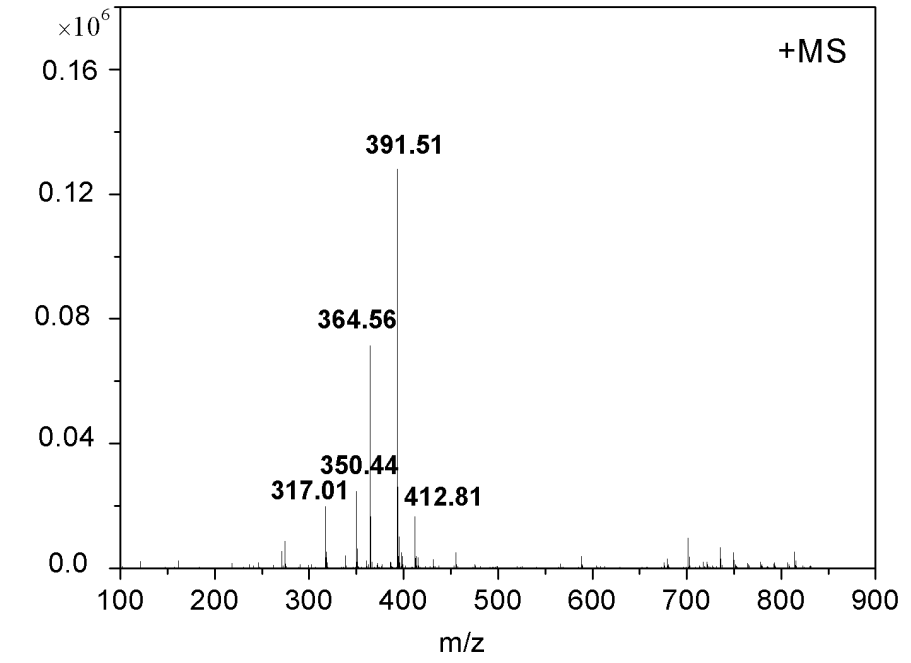

Figure S8. The mass spectra of **dMP** in DMSO for 0 h .

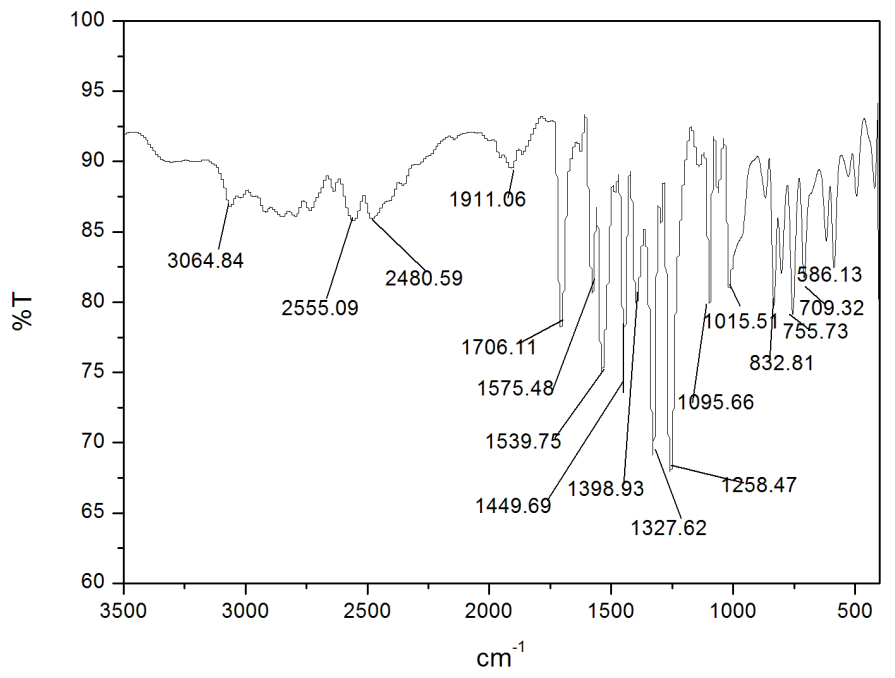

Figure S9. IR (KBr) spectra of **MP**.

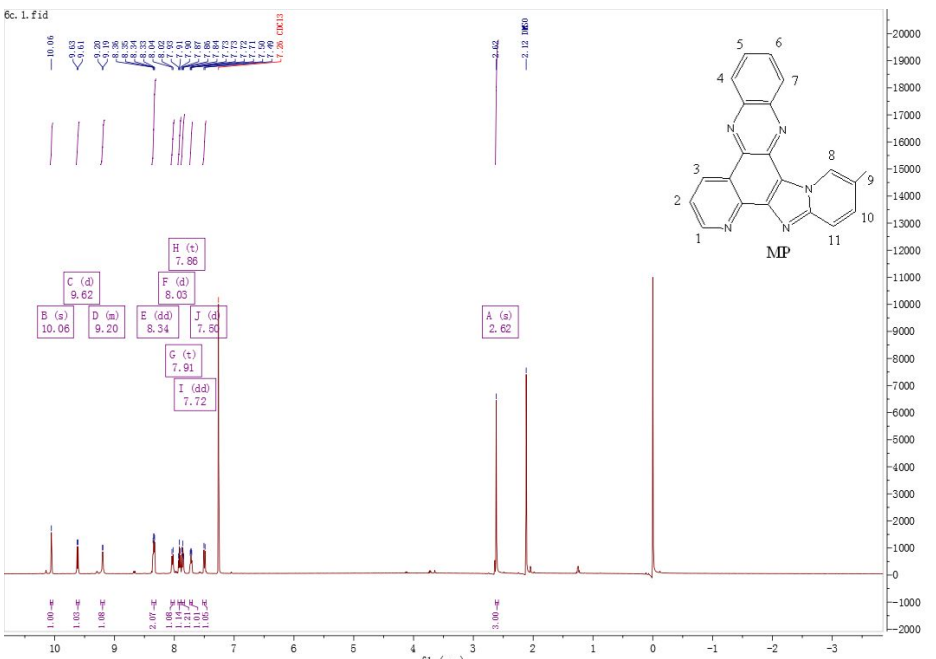

Figure S10. ^{1}H NMR (500 MHz, Chloroform-d) for **MP**

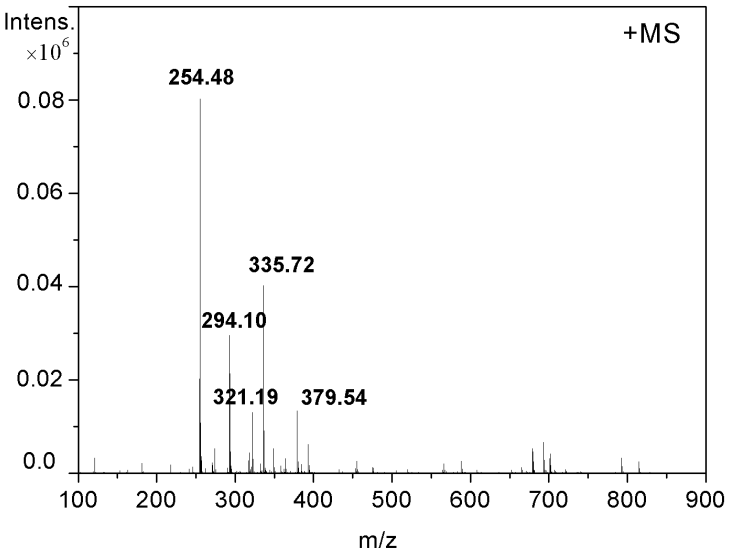

Figure S11. The mass spectra of **MP** in DMSO for 0 h .

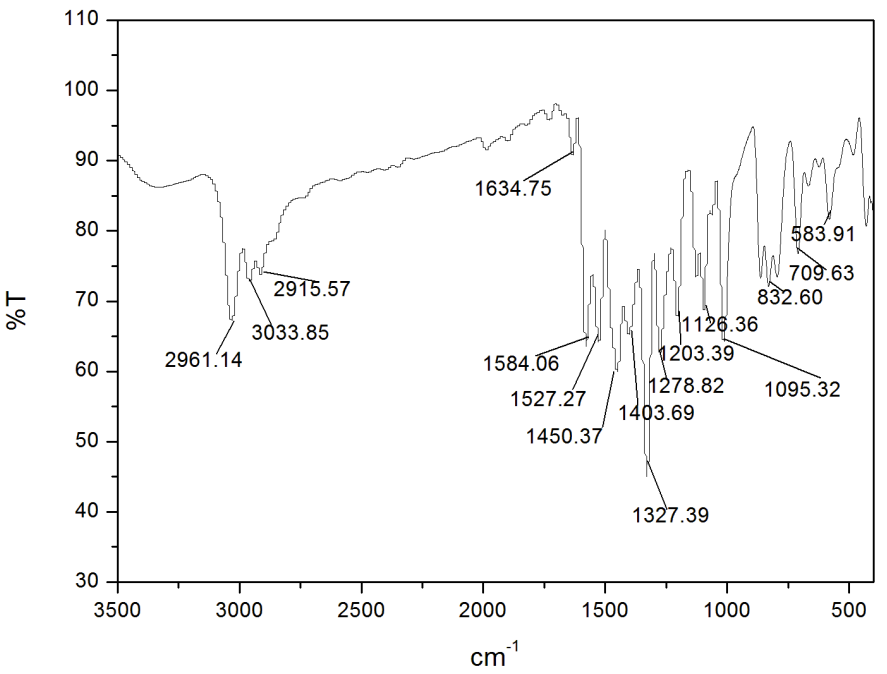

Figure S12. IR (KBr) spectra of **tMP**.

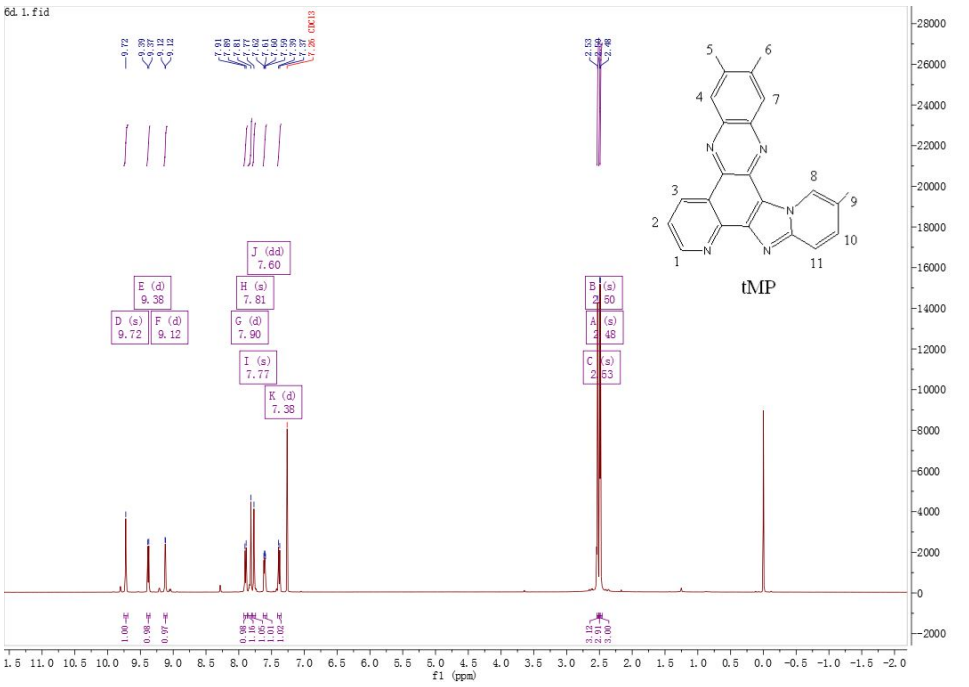

Figure S13. ^{1}H NMR (500 MHz, Chloroform-d) for **tMP**.

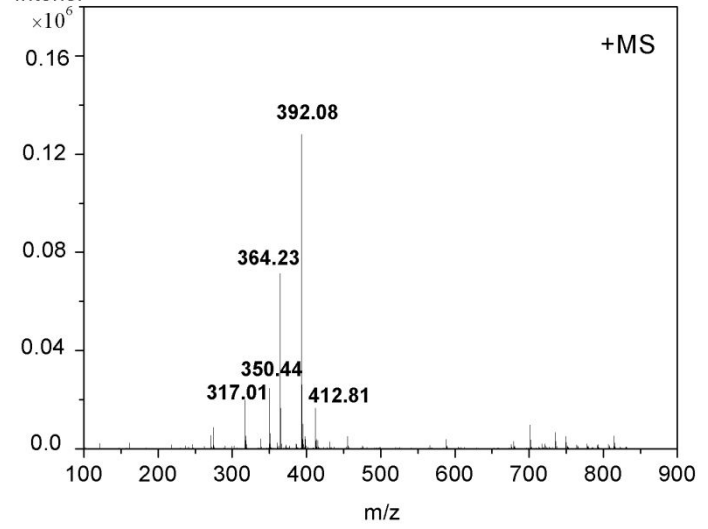

Figure S14. The mass spectra of **tMP** in DMSO for 0 h .

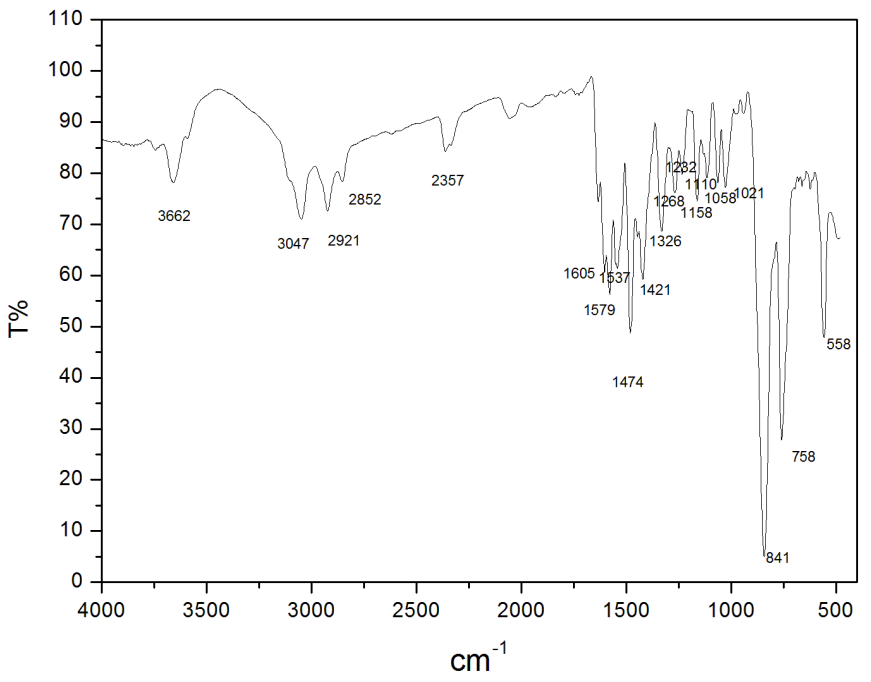

Figure S15. IR (KBr) spectra of **PyP-Ir**.

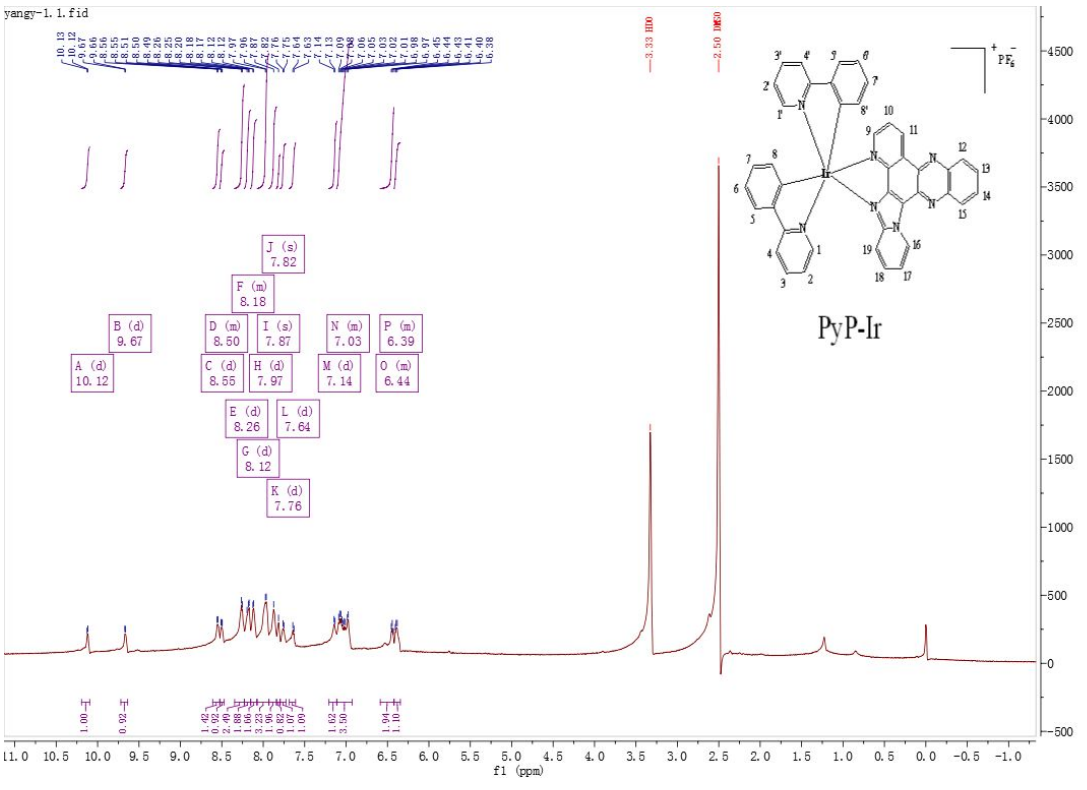

Figure S16. ^{1}H NMR (500MHz, DMSO-d_6) for **PyP-Ir**.

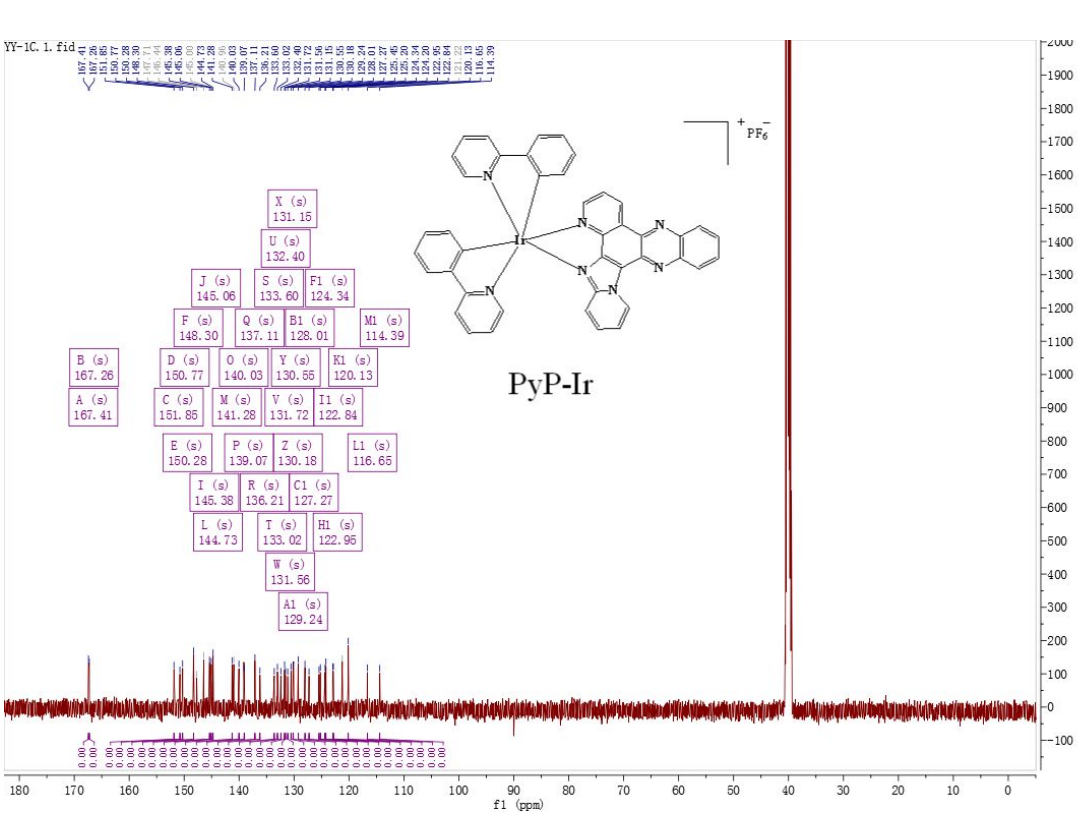

Figure S17. ^{13}C NMR (126MHz, DMSO-d_6) for **PyP-Ir**.

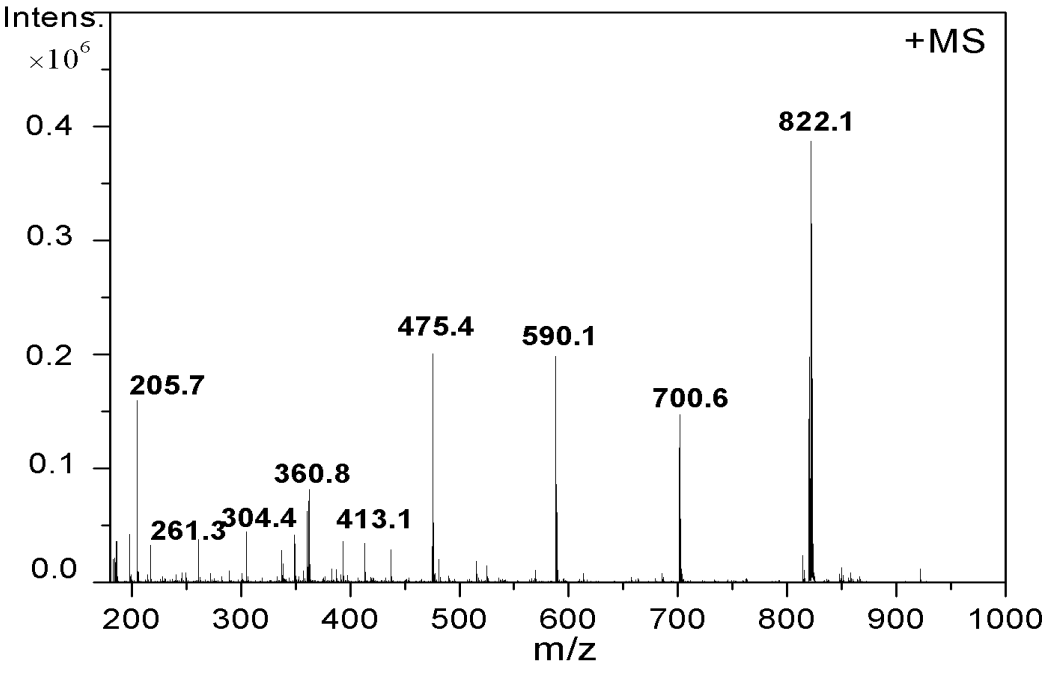

Figure S18. The mass spectra of **PyP-Ir** in DMSO for 0 h .

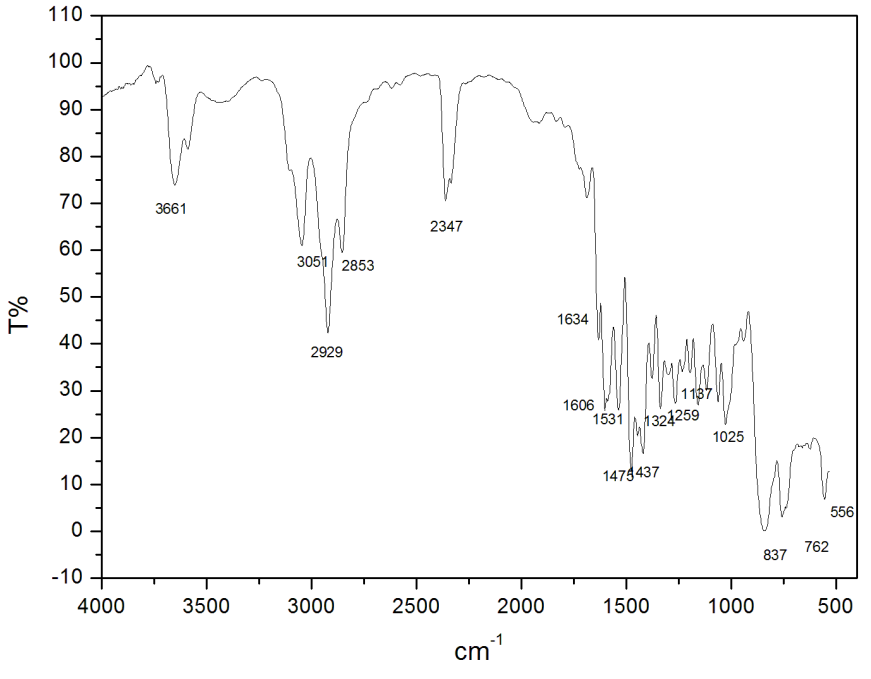

Figure S19. IR (KBr) spectra of **PydMP-Ir**.

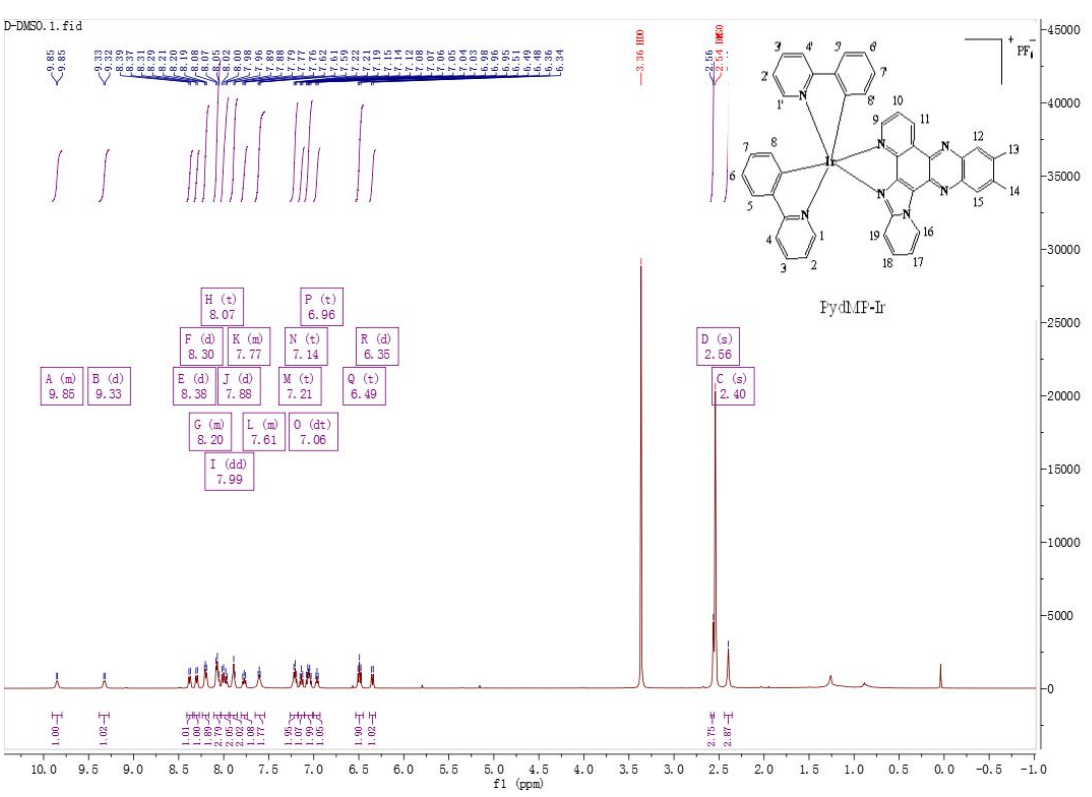

Figure S20. ^{1}H NMR (500MHz, DMSO-d_6) for **PydMP-Ir**.

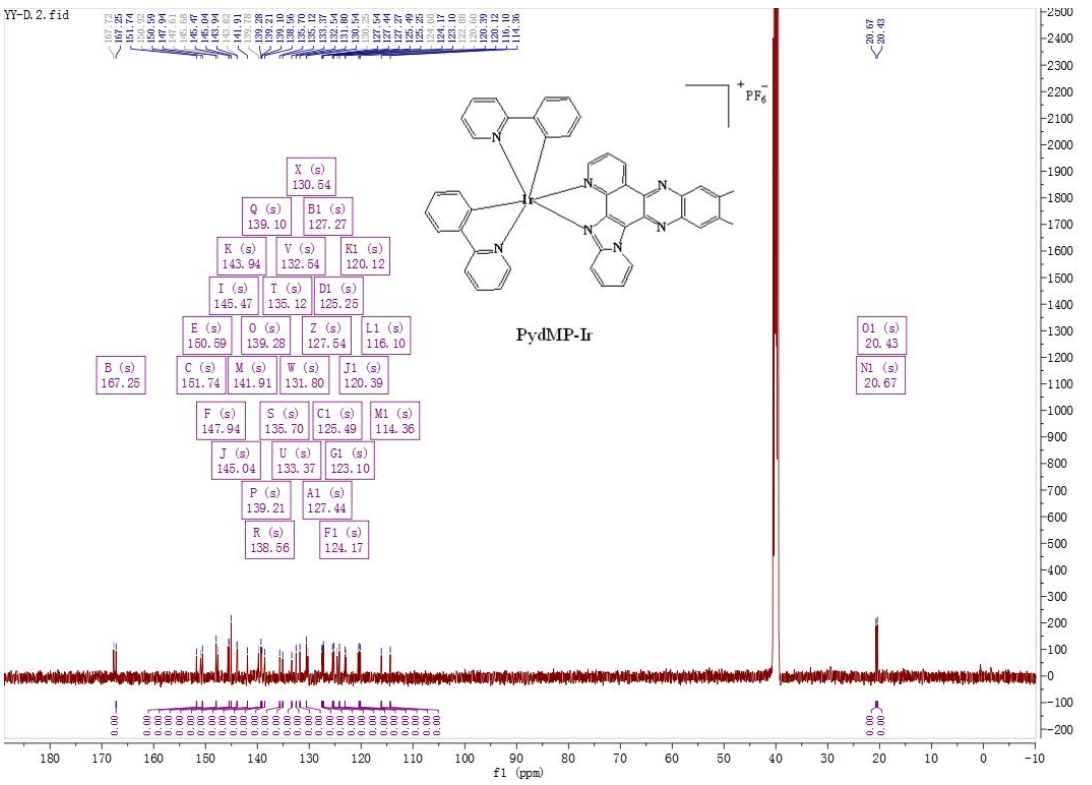

Figure S21. ^{13}C NMR (126MHz, DMSO-d_6) for **PydMP-Ir**.

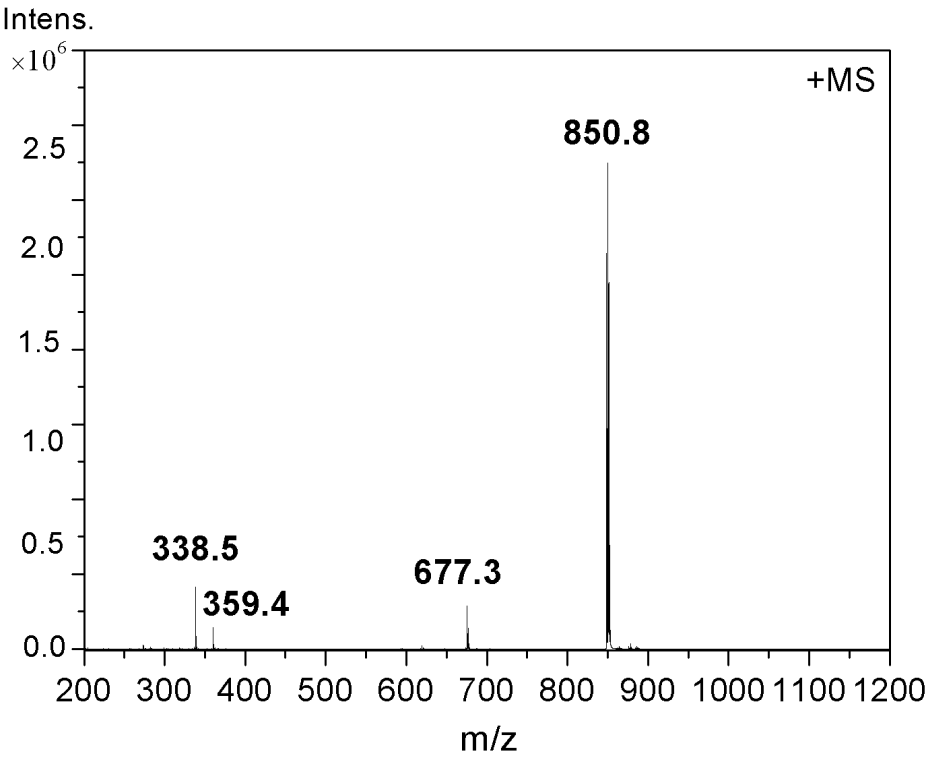

Figure S22. The mass spectra of **PydMP-Ir** in DMSO) for 0 h.

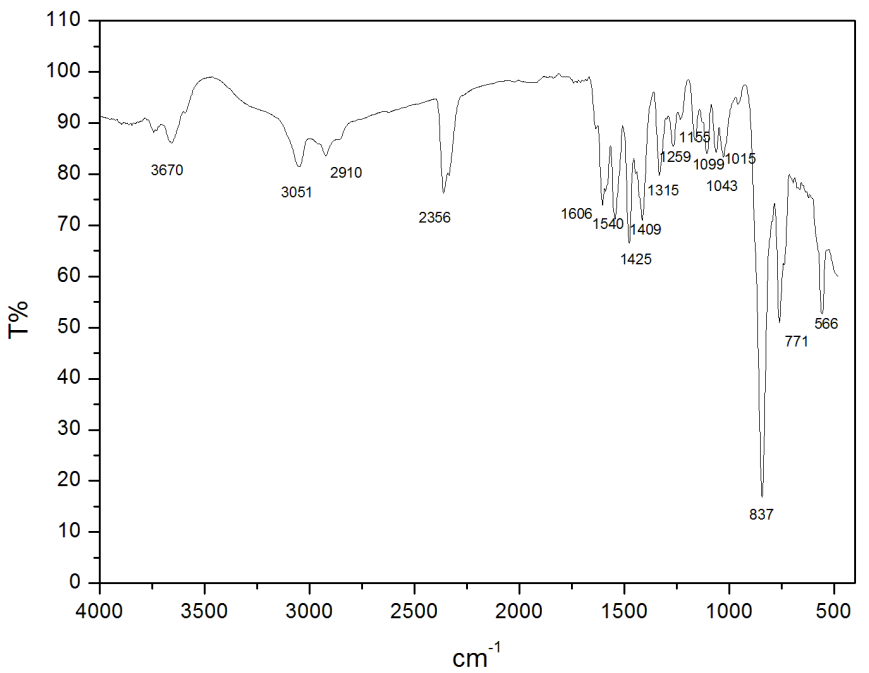

Figure S23. IR (KBr) spectra of **PyMP-Ir.**

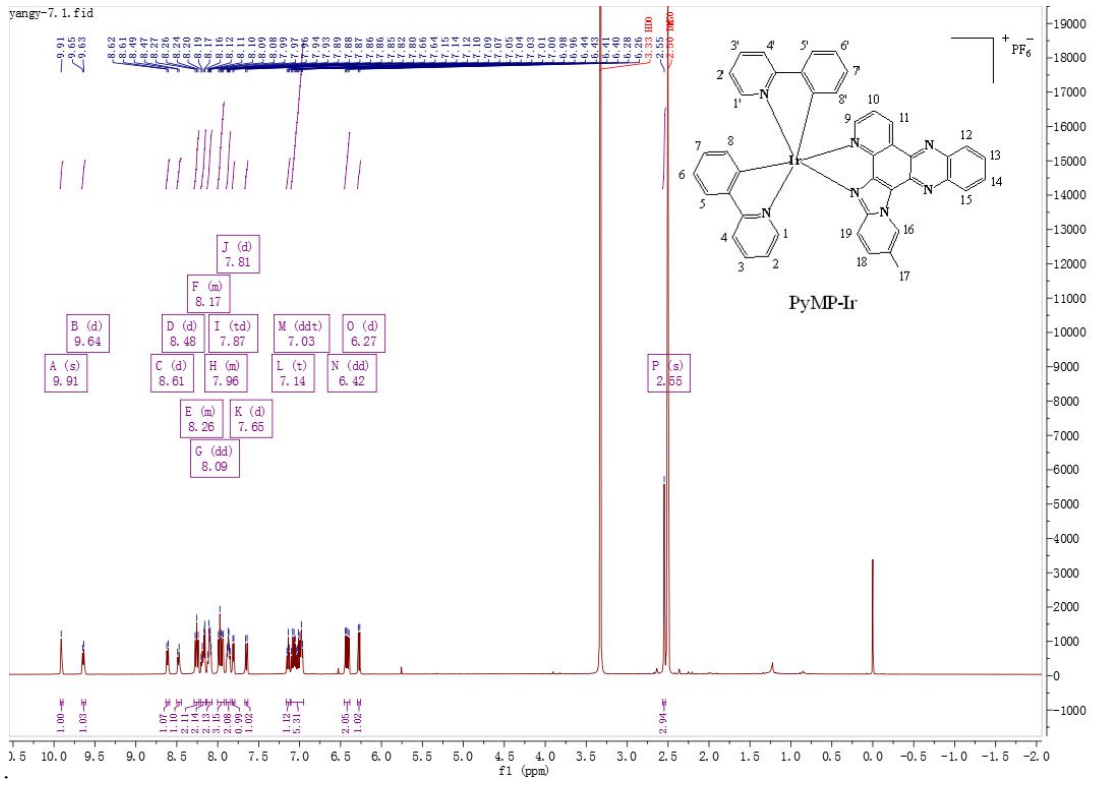

Figure S24. ^{1}H NMR (500MHz, DMSO-d_6) for **PyMP-Ir**.

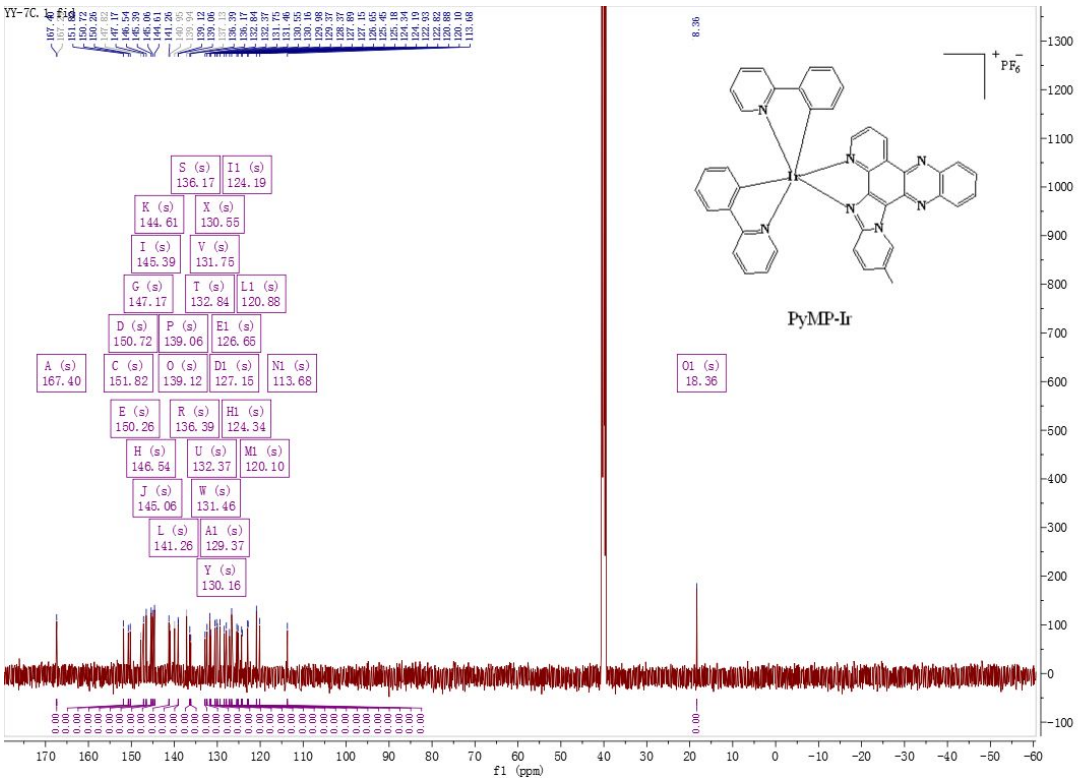

Figure S25. ^{13}C NMR (126MHz, DMSO-d_6) for **PyMP-Ir**.

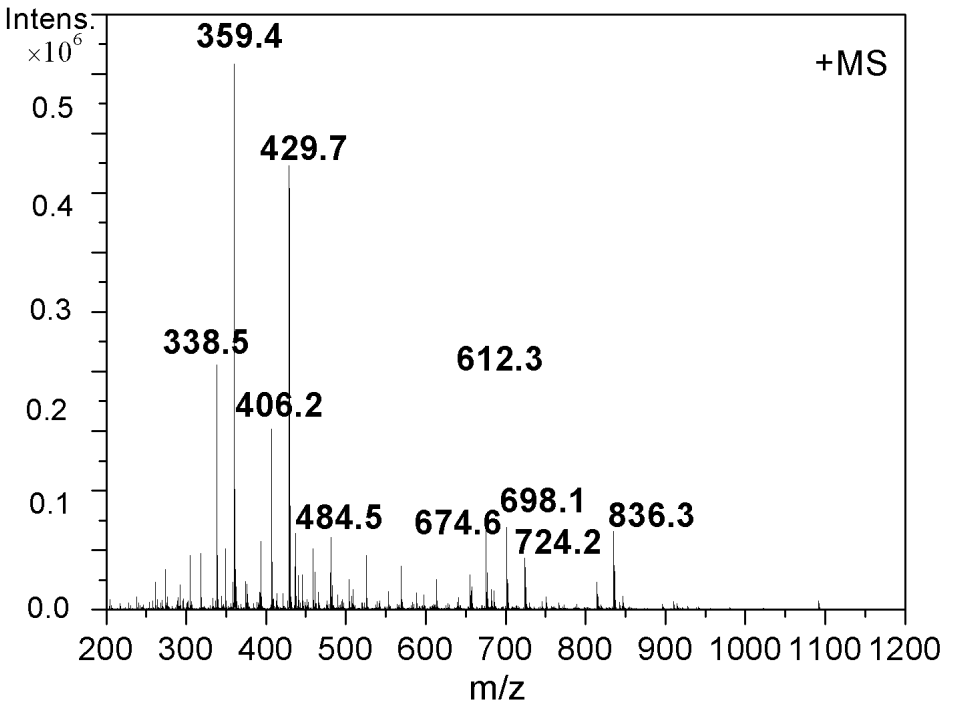

Figure S26. The mass spectra of **PyMP-Ir** in DMSO for 0 h .

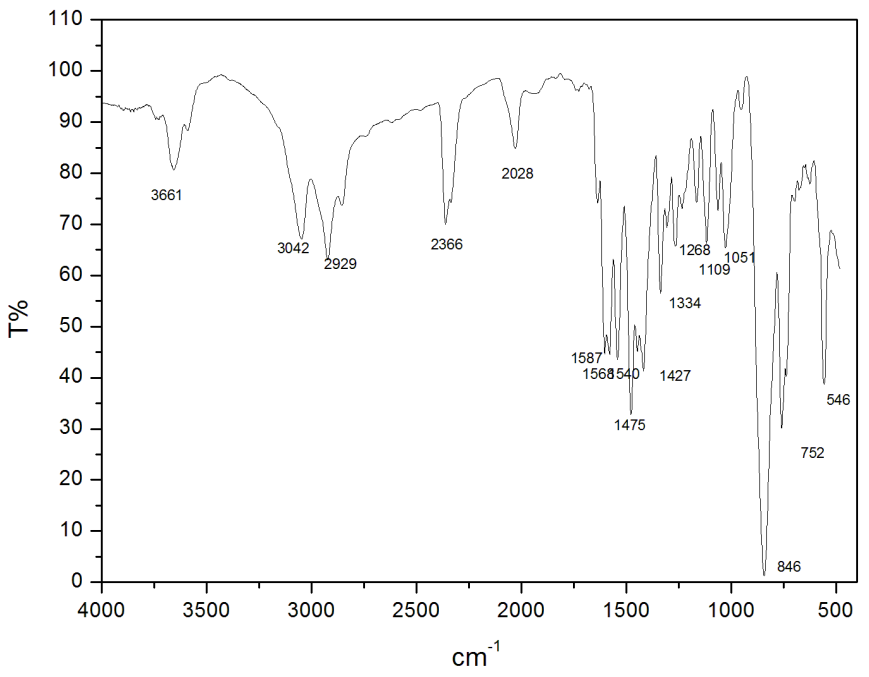

Figure S27. IR (KBr) spectra of **PytMP-Ir**.

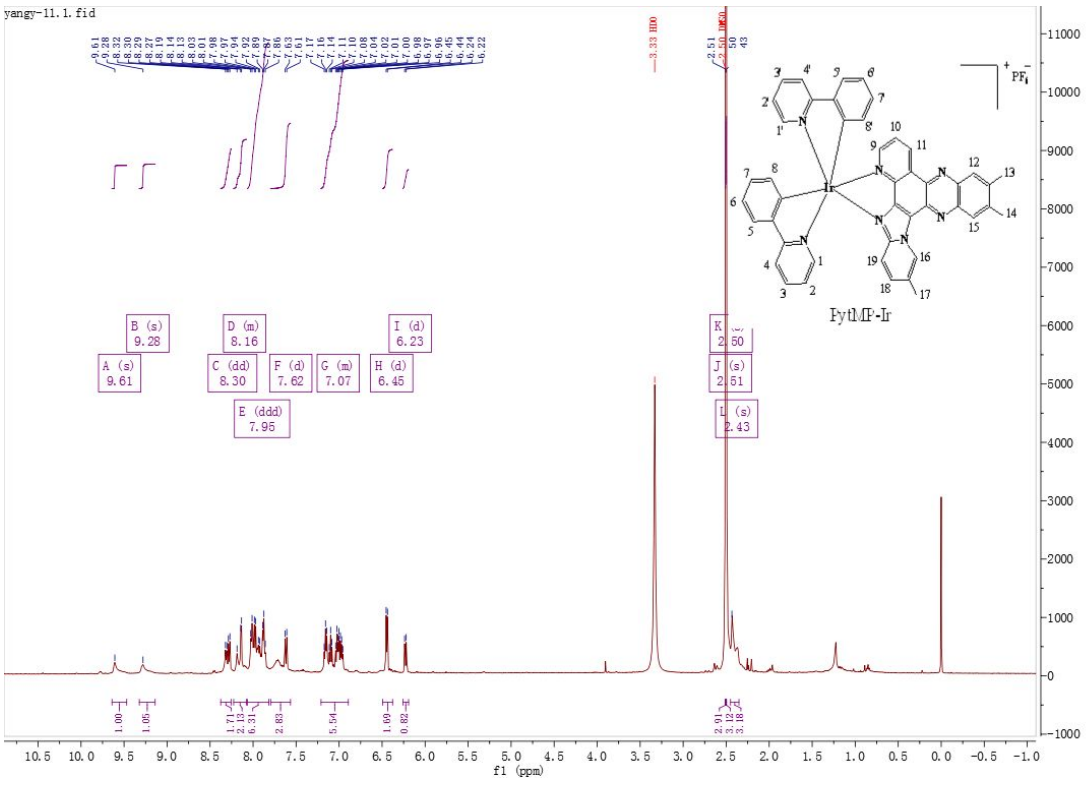

Figure S28. ^{1}H NMR (500MHz, DMSO-d_6) for **PytMP-Ir**.

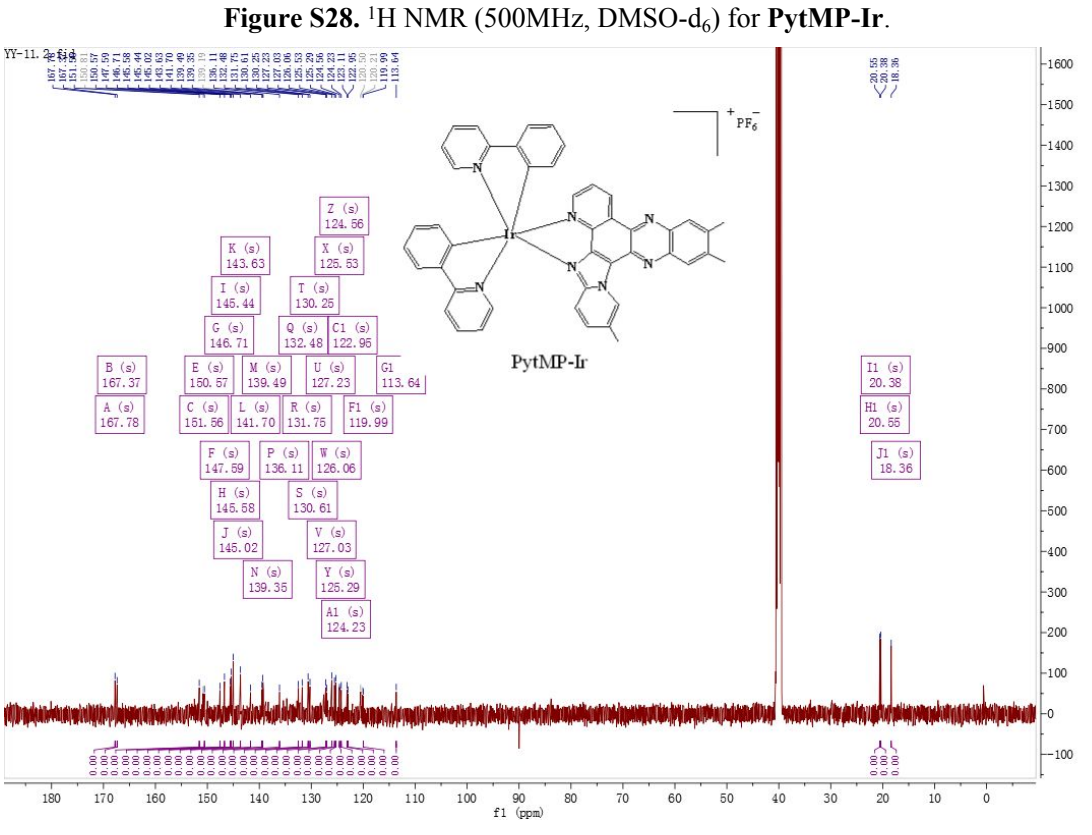

Figure S29. ^{13}C NMR (126MHz, DMSO-d_6) for **PytMP-Ir**.

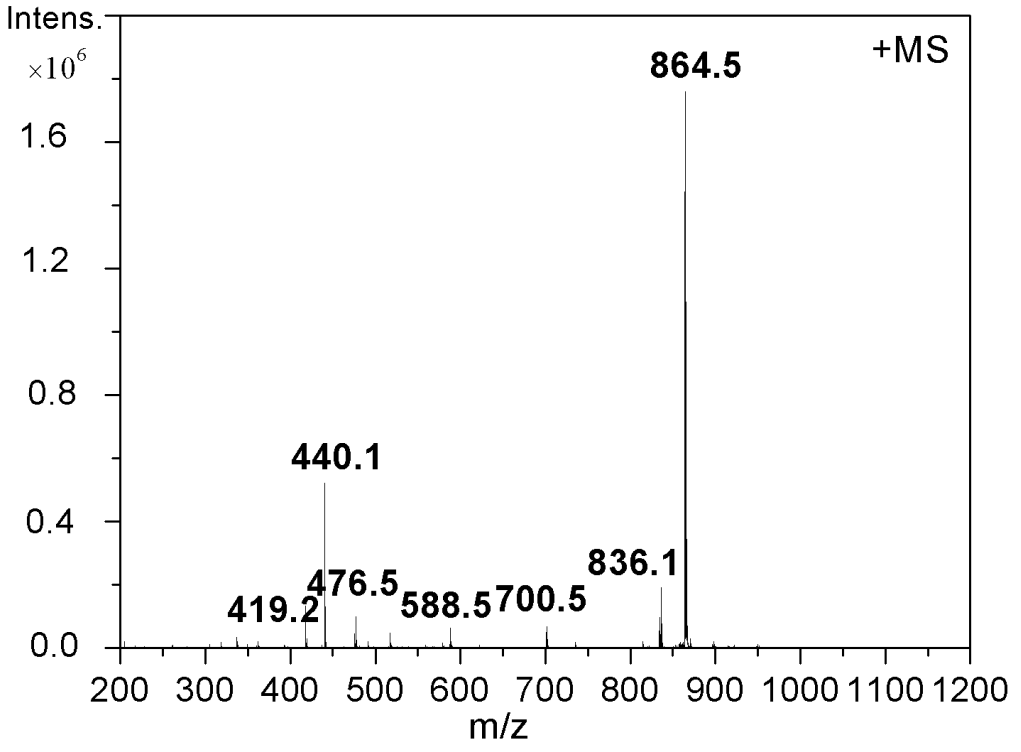

Figure S30. The mass spectra of **PytMP-Ir** in DMSO)for 0 h .

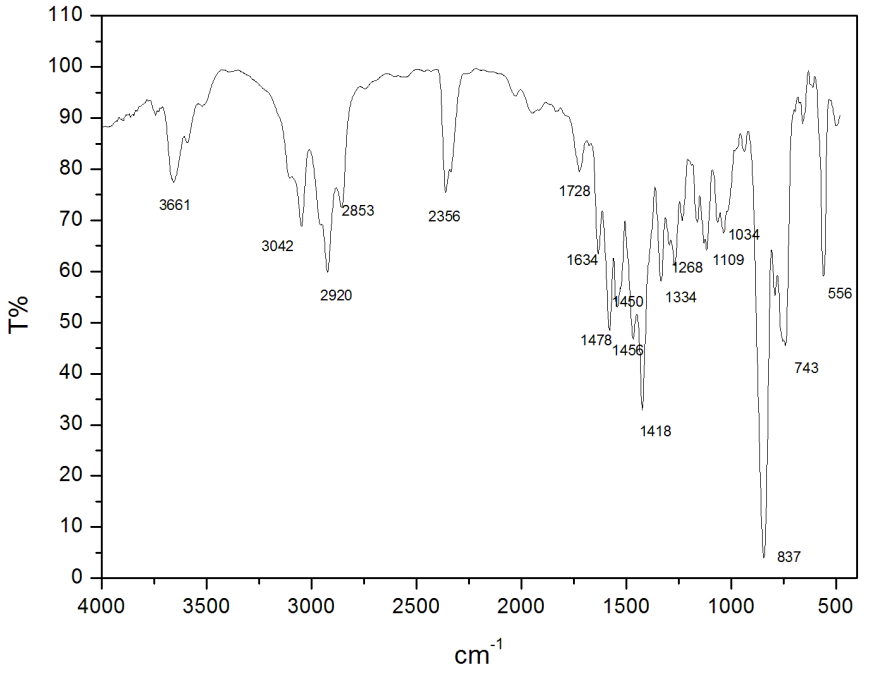

Figure S31. IR (KBr) spectra of **MPyP-Ir**.

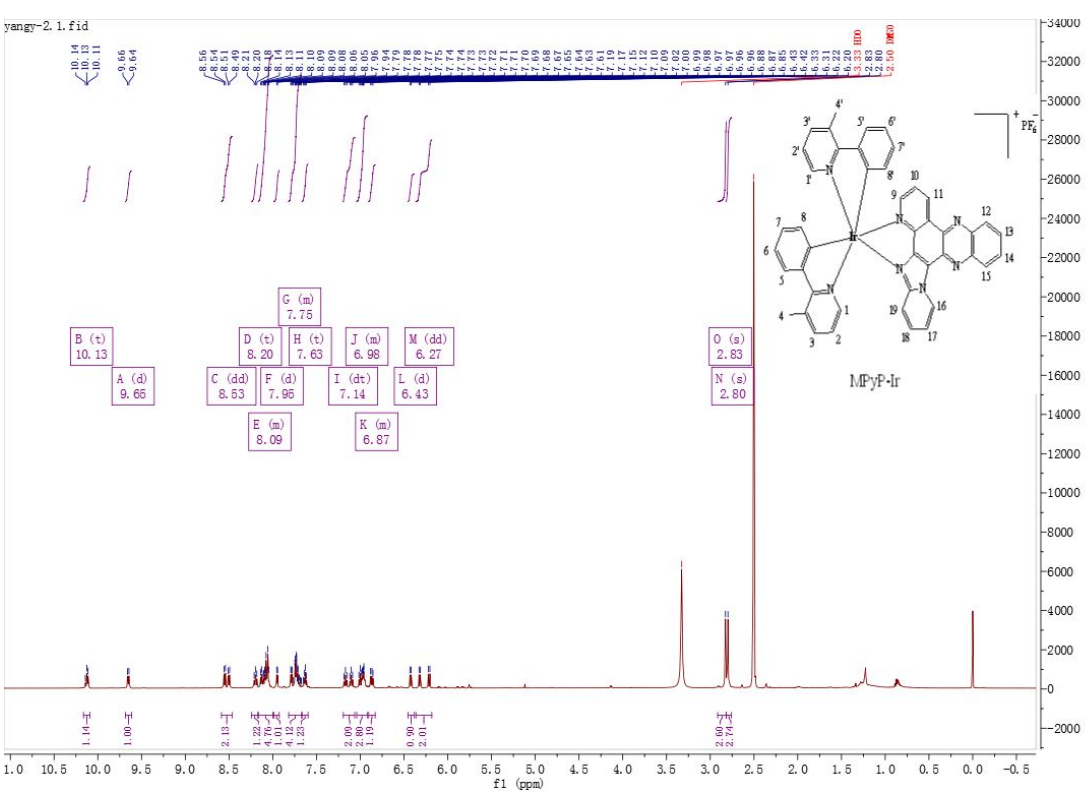

Figure S32. ^{1}H NMR (500MHz, DMSO-d_6) for **MPyP-Ir**.

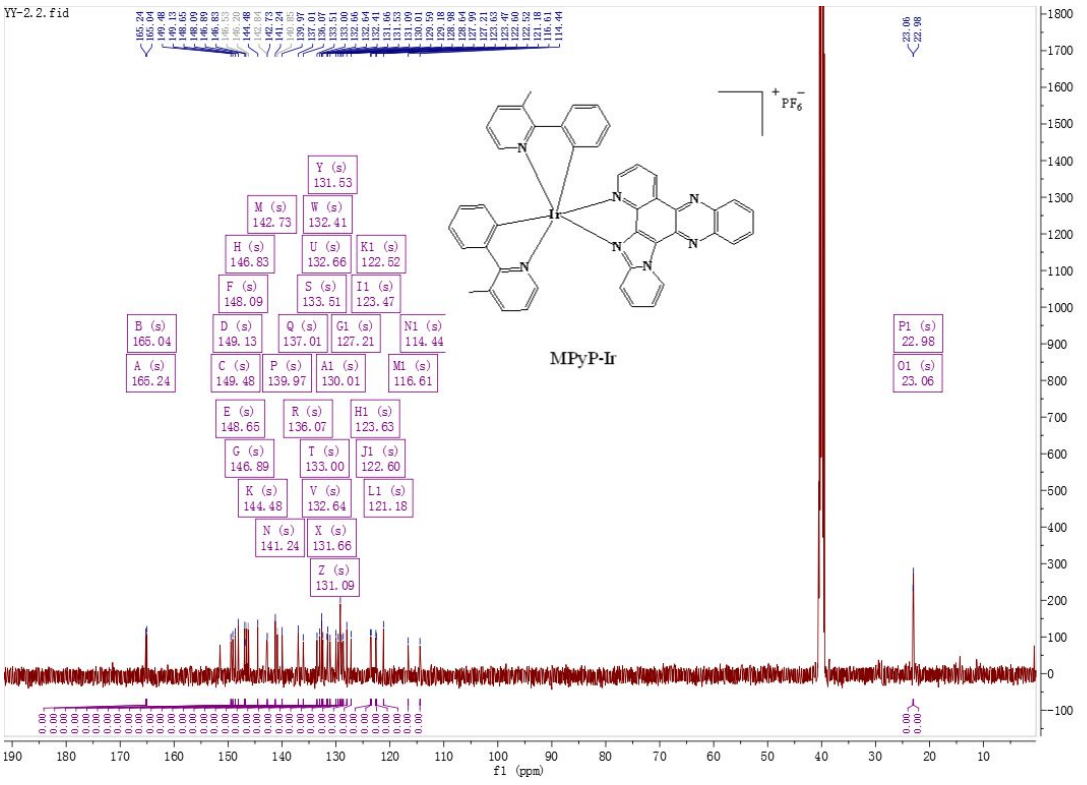

Figure S33. ^{13}C NMR (126MHz, DMSO-d_6) for **MPyP-Ir**.

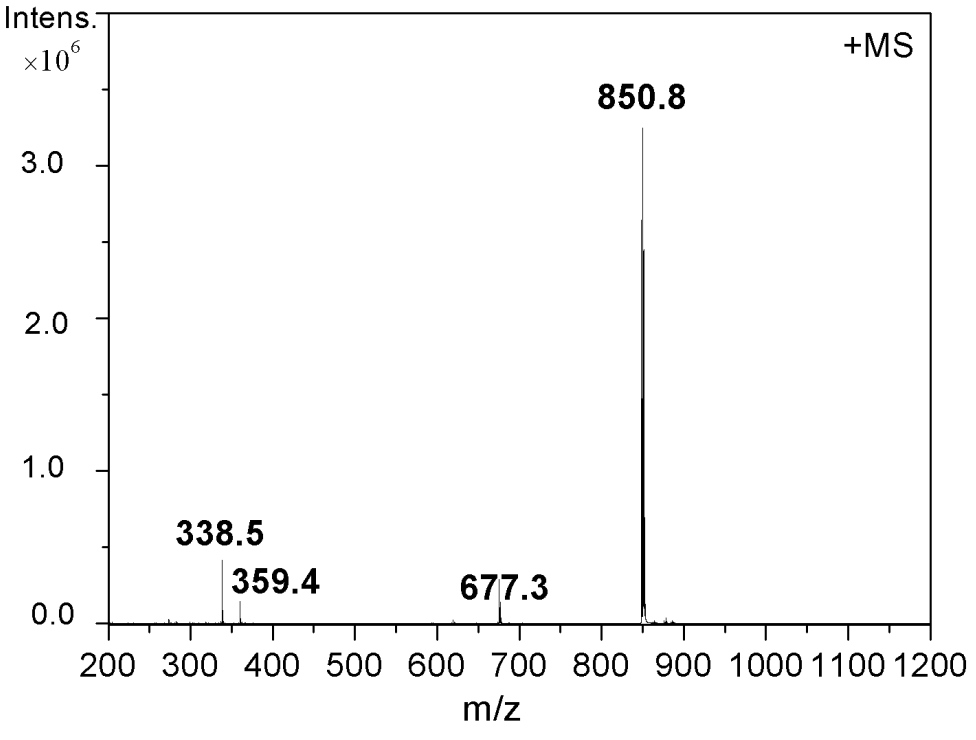

Figure S34. The mass spectra of **MPyP-Ir** in DMSO for 0 h.

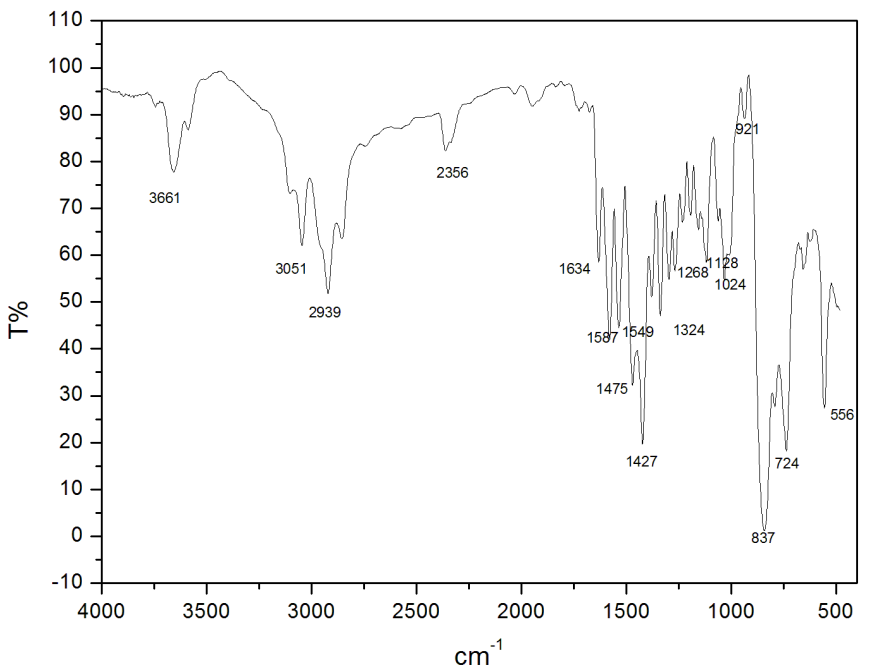

Figure S35. IR (KBr) spectra of **MPydMP-Ir**.

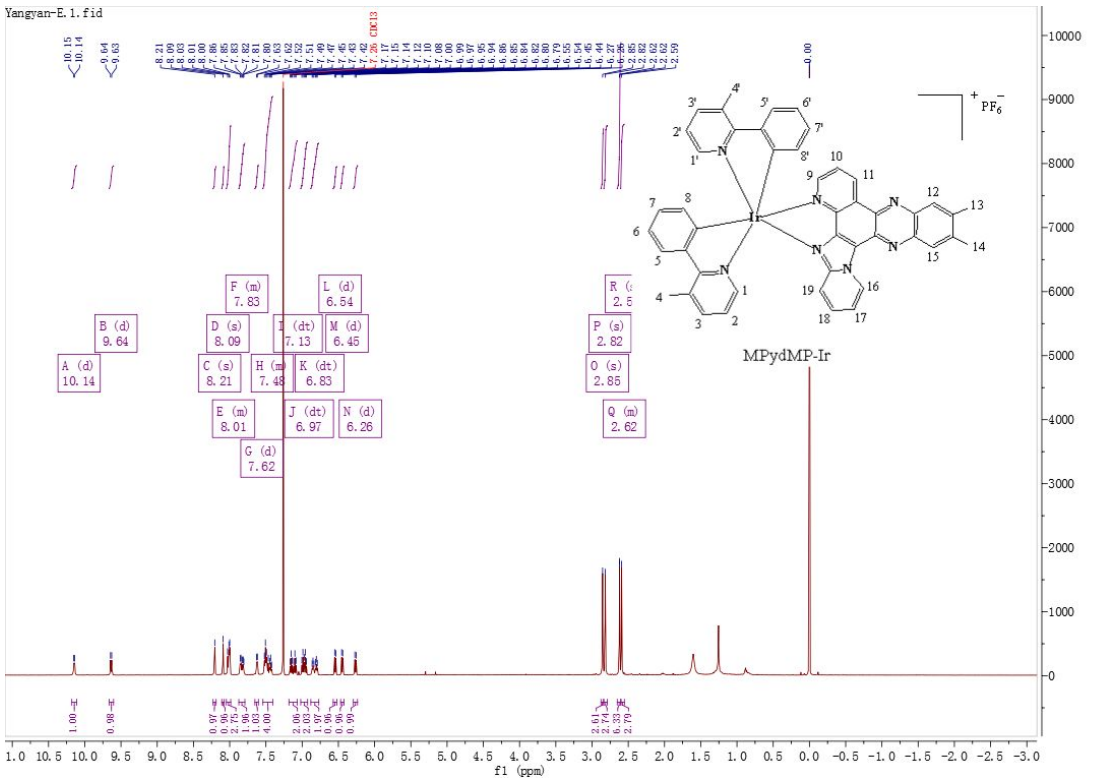

Figure S36. ^{1}H NMR (500MHz, DMSO-d_6) for **MPydMP-Ir**

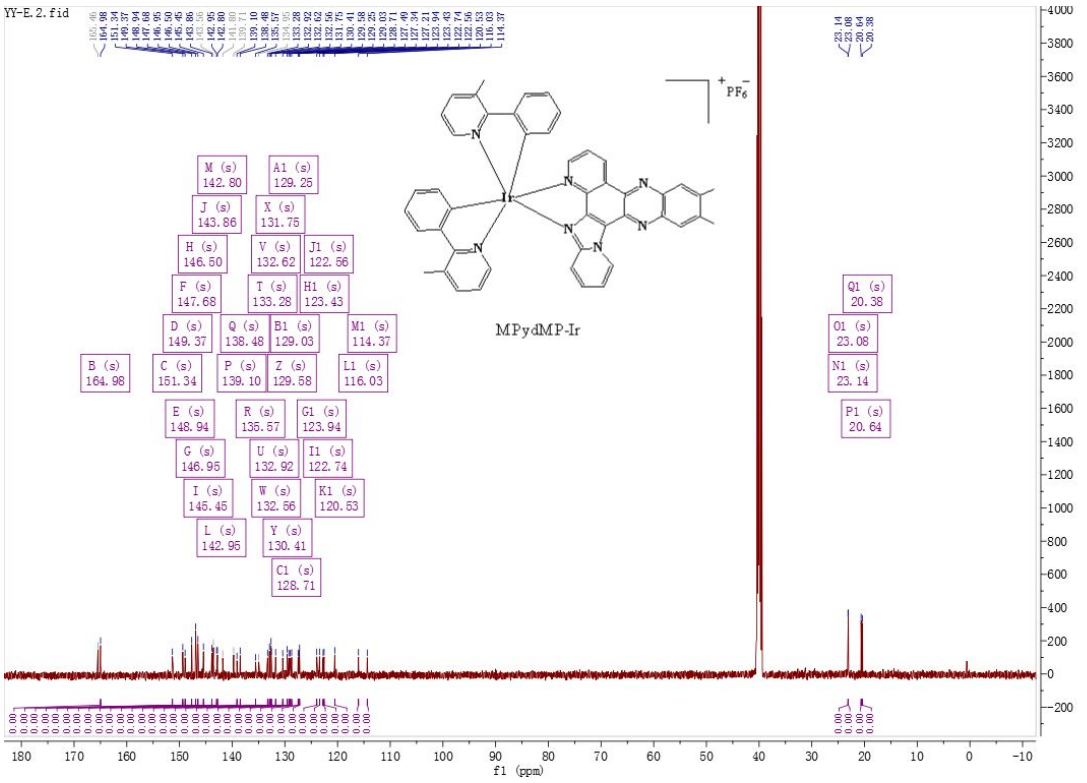

Figure S37. ^{13}C NMR (126MHz, DMSO-d_6) for **MPydMP-Ir**.

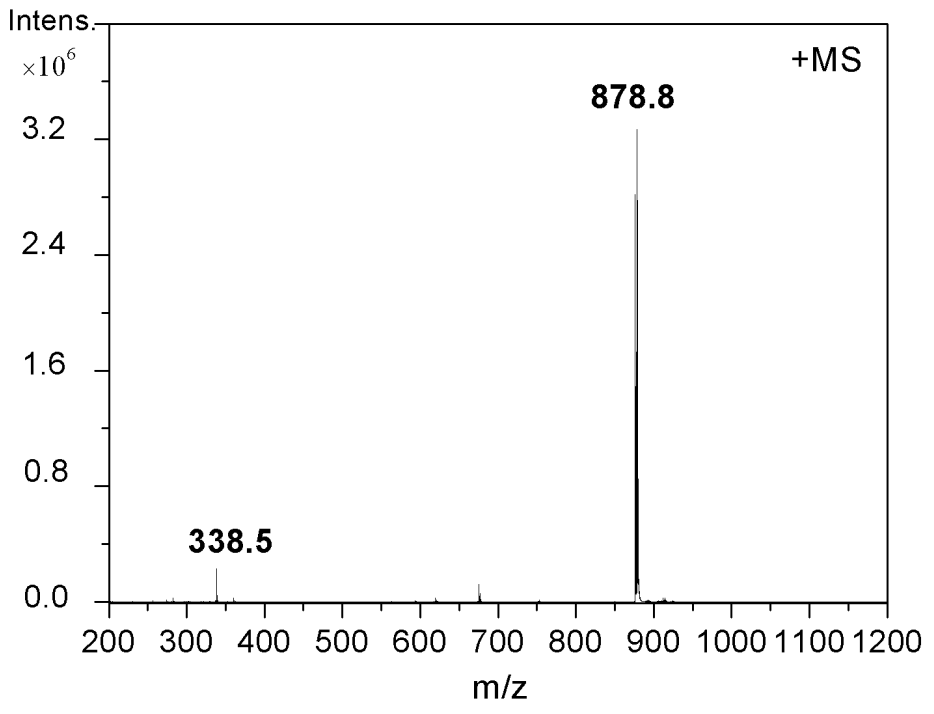

Figure S38. The mass spectra of **MPydMP-Ir** in DMSO for 0 h .

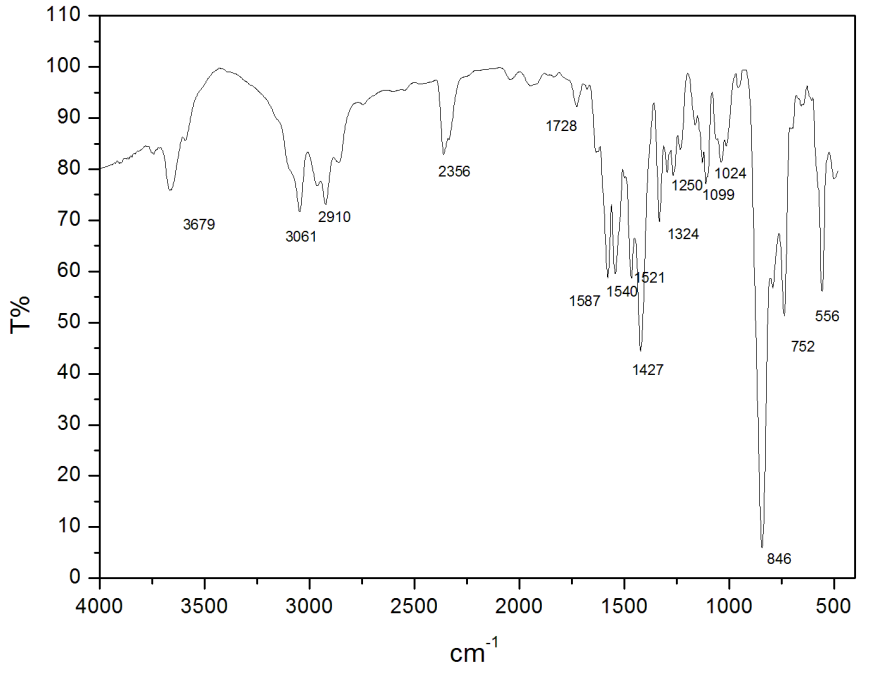

Figure S39. IR (KBr) spectra of **MPyMP-Ir**.

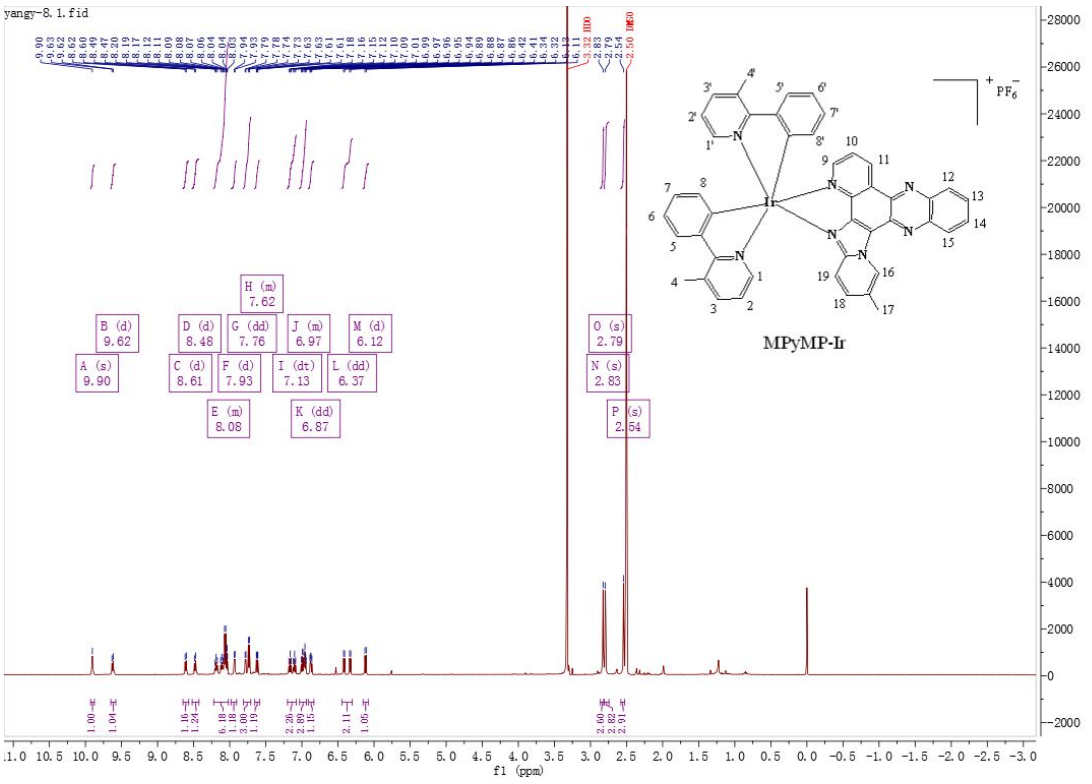

Figure S40. ^{1}H NMR (500MHz, DMSO-d_6) for **MPyMP-Ir**.

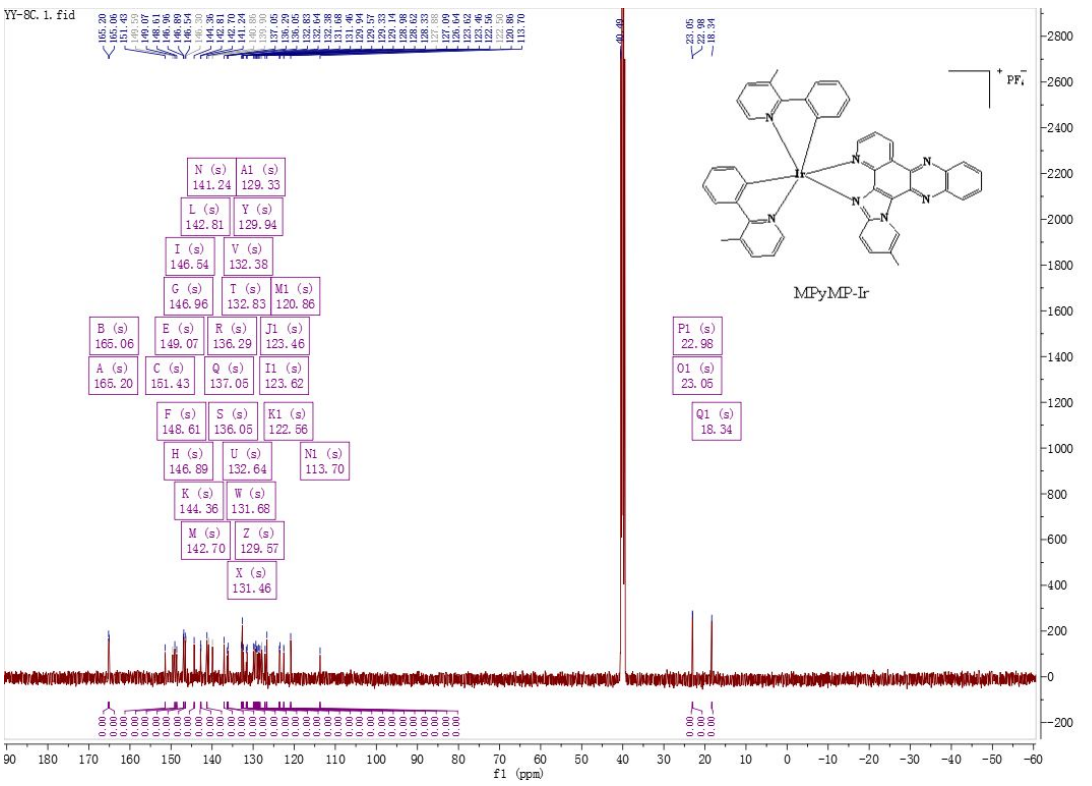

Figure S41. ^{13}C NMR (126MHz, DMSO-d_6) for **MPyMP-Ir**.

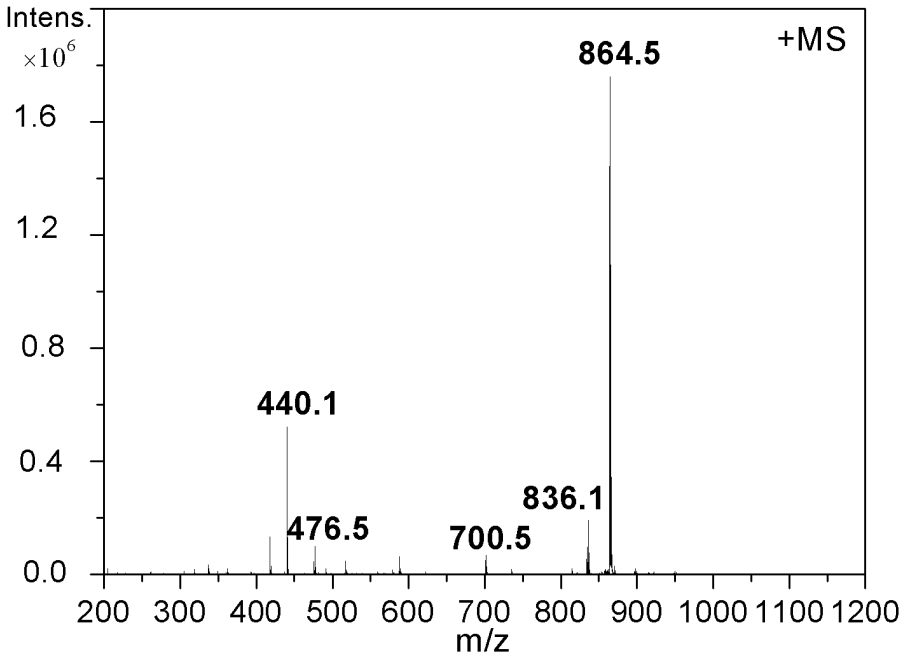

Figure S42. The mass spectra of **MPyMP-Ir** in DMSO for 0 h.

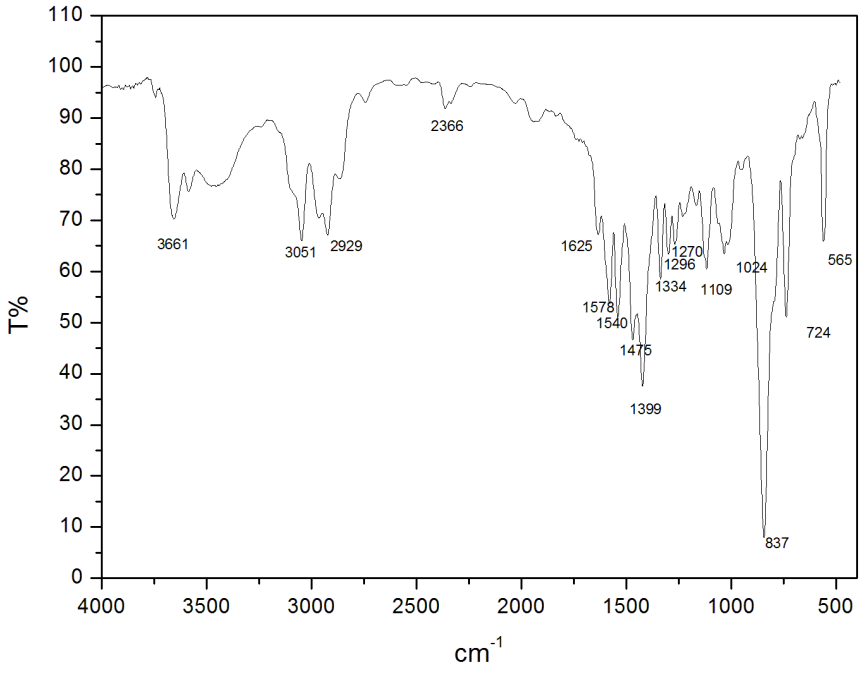

Figure S43. IR (KBr) spectra of **MPytMP-Ir**.

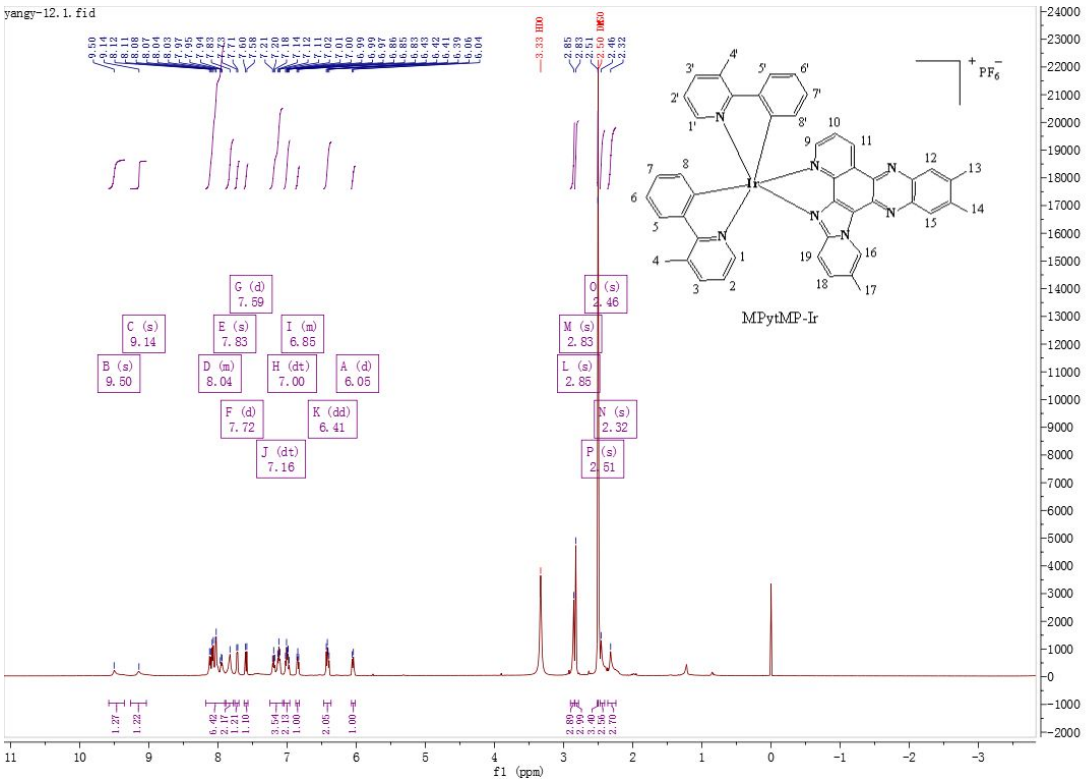

Figure S44. ^{1}H NMR (500MHz, DMSO-d_6) for **MPytMP-Ir**

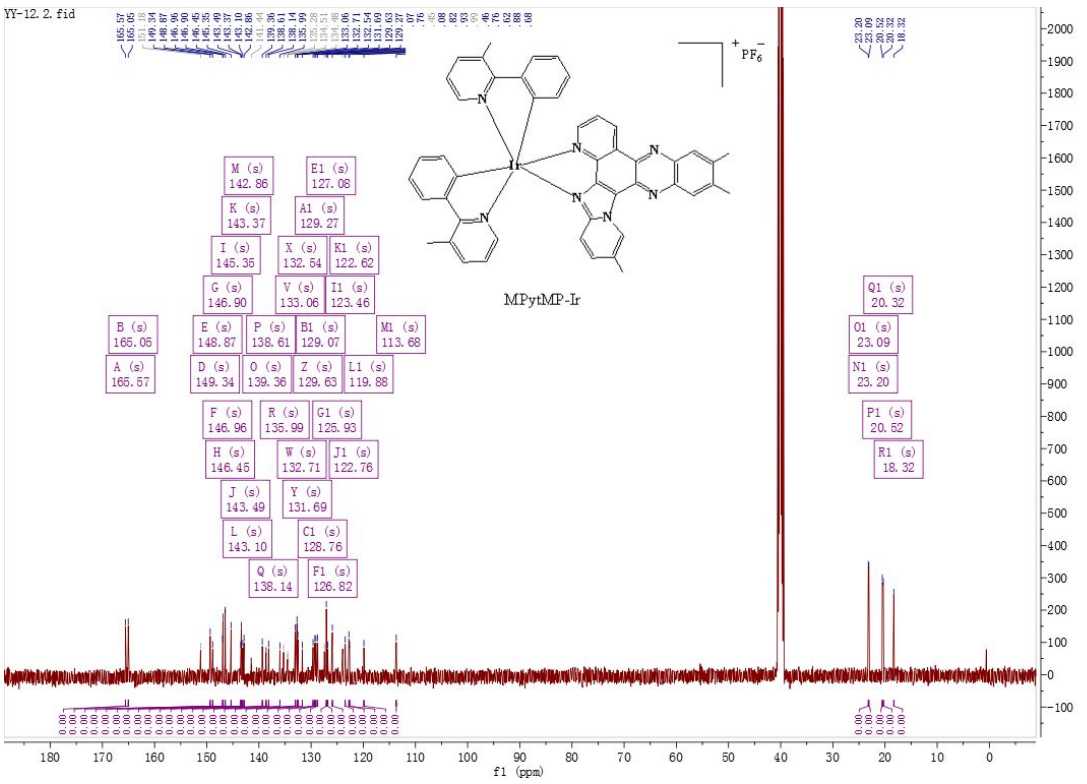

Figure S45. ^{13}C NMR (126MHz, DMSO-d_6) for **MPytMP-Ir**.

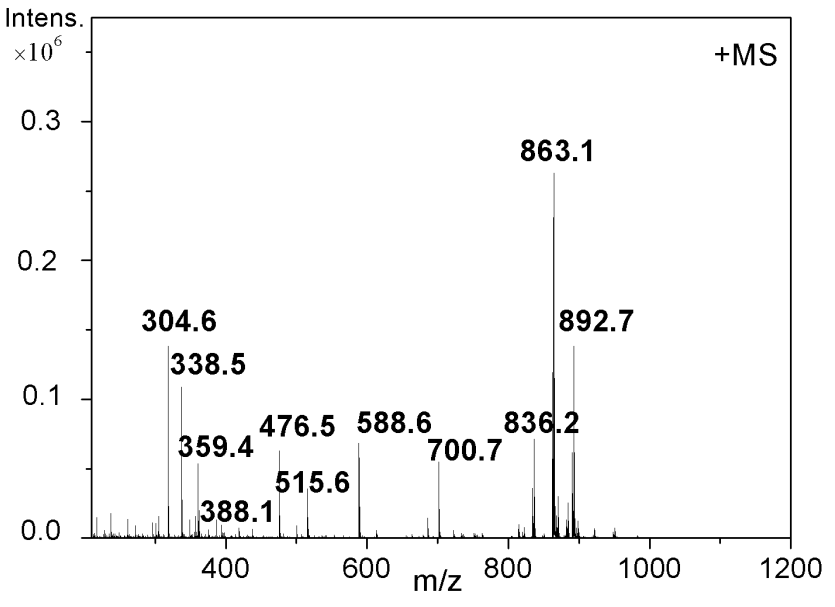

Figure S46. The mass spectra of **MPytMP-Ir** in DMSO for 0 h.

Figure S47. HPLC spectra (Waters e2695) for **MPytMP-Ir** (2.0×10^{-3} M) in Tris-HCl buffer (10 mM, pH=7.30) with 0 h (up) and 48.0 h (down). Column: Inertsustain C18 column (Waters e2695, 2998 PDA Detector HPLC COLUMN, 150 mm×5.0 μm I.D.). Column temperature: 37 ºC. Mobile phase: methanol/H_2O containing 0.01% TFA (95:5 methanol/H_2O). Flow rate: 0.65 mL/min. Injection concentration (Injection volume): 2.0×10^{-4} M (10 μL).

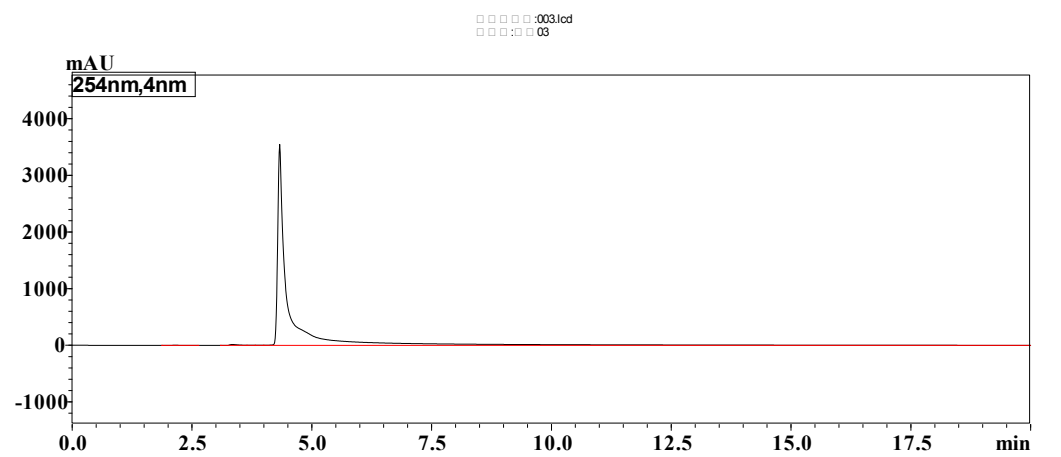

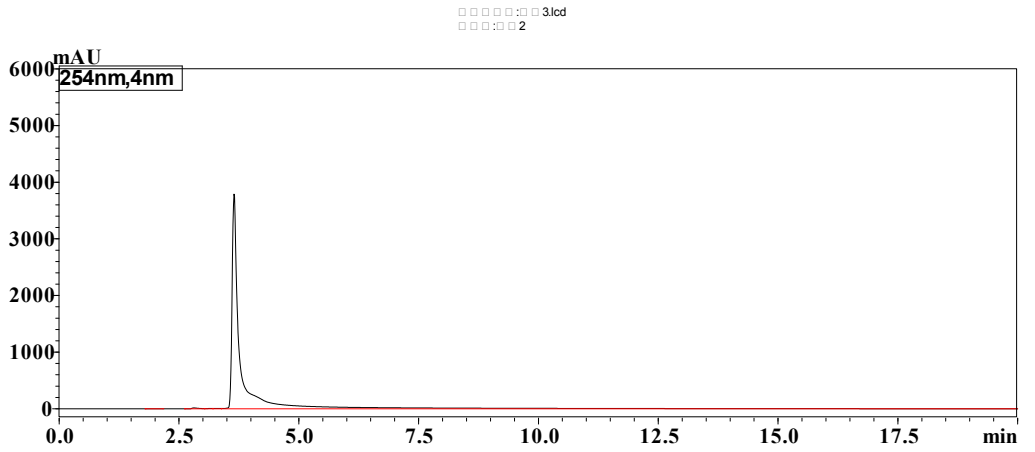

Figure S48. HPLC spectra (Waters e2695) for **MPydMP-Ir** (2.0×10^{-3} M) in Tris-HCl buffer (10 mM, pH=7.30) with 0 h (up) and 48.0 h (down). Column: Inertsustain C18 column (Waters e2695, 2998 PDA Detector HPLC COLUMN, 150 mm×5.0 μm I.D.). Column temperature: 37 ºC. Mobile phase: methanol/H_2O containing 0.01% TFA (95:5 methanol/H_2O). Flow rate: 0.65 mL/min. Injection concentration (Injection volume): 2.0×10^{-4} M (10 μL).